frontiers in Earth Science

ORIGINAL RESEARCH
published: 17 September 2021
doi: 10.3389/feart.2021.665324

Organic Molecular Paleohypsometry: A New Approach to Quantifying Paleotopography and Paleorelief

Michael T. Hren[1,2]* *and William Ouimet*[1,3]

[1]Department of Geosciences, University of Connecticut, Storrs, CT, United States, [2]Department of Chemistry, University of Connecticut, Storrs, CT, United States, [3]Department of Geography, University of Connecticut, Storrs, CT, United States

Stable isotope paleoaltimetry is one of the most commonly used approaches for quantifying the paleoelevation history of an orogen yet this methodology is often limited to arid to semi-arid climates, mountain systems with a clear orographic rainshadow and terrestrial basins. We present a new approach to reconstructing past topography and relief that uses the catchment-integrated signature of organic molecular biomarkers to quantify the hypsometry of fluvially-exported biomass. Because terrestrially-produced biomolecules are synthesized over the full range of global climate conditions and can be preserved in both terrestrial and marine sediments, the geochemistry of fluvially-transported sedimentary biomarkers can provide a means of interrogating the evolution of topography for a range of environments and depositional settings, including those not well suited for a traditional isotope paleoaltimetry approach. We show an example from Taiwan, a rapidly eroding tropical mountain system that is characterized by high rates of biomass production and short organic residence time and discuss key factors that can influence molecular isotope signal production, transport and integration. Data show that in high relief catchments of Taiwan, river sediments can record integration of biomass produced throughout the catchment. Sedimentary biomarker δ^2H_{nC29} in low elevation river deposition sites is generally offset from the δ^2H_{nC29} value observed in local soils and consistent with an isotope composition of organics produced at the catchment mean elevation. We test the effect of distinct molecular production and erosion functions on the expected δ^2H_{nC29} in river sediments and show that elevation-dependent differences in the production and erosion of biomarkers/sediment may yield only modest differences in the catchment-integrated isotopic signal. Relating fluvial biomarker isotope records to quantitative estimates of organic source elevations in other global orogens will likely pose numerous challenges, with a number of variables that influence molecular production and integration in a river system. We provide a discussion of important parameters that influence molecular biomarker isotope signatures in a mountain system and a framework for employing a molecular paleohypsometry approach to quantifying the evolution of other orogenic systems.

Keywords: paleoelevation, paleotopography, stable isotopes, biomarker, catchment integration

OPEN ACCESS

Edited by:
Paolo Ballato,
Roma Tre University, Italy

Reviewed by:
Yan Bai,
Center for Excellence in Tibetan Plateau Earth Science (CAS), China
Joel Saylor,
University of British Columbia, Canada

***Correspondence:**
Michael T. Hren
michael.hren@uconn.edu

Specialty section:
This article was submitted to Quaternary Science, Geomorphology and Paleoenvironment, a section of the journal Frontiers in Earth Science

Received: *07 February 2021*
Accepted: *30 August 2021*
Published: *17 September 2021*

Citation:
Hren MT and Ouimet W (2021) Organic Molecular Paleohypsometry: A New Approach to Quantifying Paleotopography and Paleorelief. Front. Earth Sci. 9:665324. doi: 10.3389/feart.2021.665324

INTRODUCTION

The development of large orogens can produce fundamental shifts in global physical and chemical fluxes, atmospheric dynamics, biologic change, and even long-term changes in the redox state of the mantle (Kutzbach et al., 1989; Ruddiman and Kutzbach, 1989; Ramstein et al., 1997; Ruddiman, 2013). Records of the paleoelevation history of an orogen or the evolution of orogenic relief are critical for quantifying the feedbacks among climate, erosion and tectonics, yet challenging to produce. As a result, developing reliable records of paleotopography remains one of the grand challenges in the Earth sciences (National Academies of Sciences, Engineering, and Medicine et al., 2020).

Over the past 20 years, numerous approaches have been developed to quantify changes in the topography of an orogen (Axelrod, 1997; Forest et al., 1999; Garzione et al., 2000; Poage and Chamberlain, 2001; Poage and Chamberlain, 2002; Sahagian et al., 2002; Ghosh et al., 2006; Rowley, 2006/8; Clark, 2007; Rowley and Garzione, 2007; Sahagian and Proussevitch, 2007; Hren et al., 2010). Yet, there continues to be a fundamental information gap with regard to approaches for quantifying topographic change for numerous types of orogens. In particular, current methodologies are commonly limited to application in systems that are characterized by simple orographic rainshadows and a semi-arid to arid climate, terrestrial foreland basin systems, and temperate to cool terrestrial settings with mild to moderate chemical weathering rates. There remain few paleotopography reconstruction approaches that are successful for wet, tropical mountain belts with complex climatology and moisture sourcing, or systems with predominantly marine deposition.

Here we discuss a new approach to quantifying the paleohypsometry of an orogen using the stable isotope composition of organic molecular biomarkers that are produced within a catchment and exported via river networks. This approach is similar to the time-tested methods of cosmogenic isotope determination of catchment erosion rate (Bierman, 1994; Bierman and Steig, 1996; Granger et al., 1996; Heimsath et al., 2001). Specifically, in an evolving orogen, organic biomass may be produced throughout a catchment. As an orogen and associated catchments evolve, distinct elevation and precipitation isotope and temperature patterns emerge for all points in the catchment. Biomolecules produced by plants or microorganisms at each point in the landscape can record the signature of precipitation isotopes or temperature at the point of production. These molecules are incorporated into soils, bound to clay particles and mobilized throughout a catchment. The geochemical signature of fluvial sediments sampled along the length of a river profile should therefore reflect changes in the source areas of contributing sediment. If the molecular production function and catchment-wide biomass integration can be characterized, the geochemical record preserved in exported and buried sediments can be used to derive a catchment-specific signature of topography and relief through time.

This method focuses on geochemical signatures preserved in material exported from an orogen through river networks. While there are a host of process-specific relationships to resolve for different climate and erosion regimes, the potential power of this approach is that it greatly expands the possible range of sediments that quantitatively capture orogenic events and provides a template for producing measures of catchment hypsometry through time.

Stable Isotope Paleoaltimetry

There are a number of approaches that have been developed to constrain paleotopography (e.g., Kohn, 2018 and references therein). These generally rely on environmental variables that are related to elevation such as temperature (Quade et al., 2013; Quade et al., 2007), pressure (Sahagian and Maus, 1994; Sahagian et al., 2002; Sahagian and Proussevitch, 2007), plant physiology (Wolfe et al., 1997; Forest et al., 1999), or water isotopes (Garzione et al., 2000; Poage and Chamberlain, 2001; Poage and Chamberlain, 2002; Rowley and Garzione, 2007; Hren et al., 2009). Over the past several decades, stable isotope paleoaltimetry has become one of the most commonly utilized paleoelevation techniques (e.g., Huntington et al., 2015; Wheeler et al., 2016; Fan et al., 2017; Tang et al., 2017; Bershaw et al., 2019; Li et al., 2019; Zhuang et al., 2019). This is due in part, to the abundance of materials that preserve the isotopic signature of ambient water such as carbonates and clays (Chamberlain and Poage, 2000; Sjostrom et al., 2006; Mulch and Chamberlain, 2007; Mulch et al., 2007), volcanic glasses (Cassel et al., 2009; Bershaw et al., 2019; Colwyn et al., 2019; Colwyn and Hren, 2019), fossils (Kohn et al., 2002), and leaf waxes (Polissar et al., 2009; Hren et al., 2010; Anderson et al., 2015; Zhuang et al., 2019). Application of stable isotope-based approaches has provided fundamental insight into how Cordilleran orogens evolve (Fan et al., 2017; Feng et al., 2013; Kent-Corson et al., 2006; Andreas Mulch and Chamberlain, 2007), long-timescale changes in the elevation of orogenic plateaus (Dettman et al., 2003; Ghosh et al., 2006; Molnar et al., 2006; Rowley and Currie, 2006; Hoke et al., 2014; Currie et al., 2016), even the role of tectonic change on biological diversification (Phillips et al., 2013).

Stable isotope paleoaltimetry is founded on the principle that as a moist airmass encounters a topographic barrier, it can undergo lifting, cooling and rainout (Rowley et al., 2001; Rowley and Garzione, 2007; Rowley, 2007). Oxygen and hydrogen fractionation of the rainwater results from the strong temperature-dependence of isotopic partitioning between vapor and liquid or solid phases. Condensation across an orogen progressively removes the "heavy" isotope species producing a characteristic Rayleigh distillation pattern in precipitation that is often described as the isotopic "altitude effect" (Dansgaard, 1964; Gonfiantini et al., 2001) (**Figure 1**).

While frequently applied as a geochemical technique, there are several key requirements for isotope paleoaltimetry to reliably record changes to topography: 1) changes in surface topography must impart a predictable change in the isotopic composition of ambient water and/or local temperature (i.e., signal generation); 2) proxy materials that form in equilibrium with ambient waters (i.e., clays, glasses, carbonates, or organic matter) must record these changes (signal recording); and 3) proxy records of this change must be preserved in sedimentary environments in

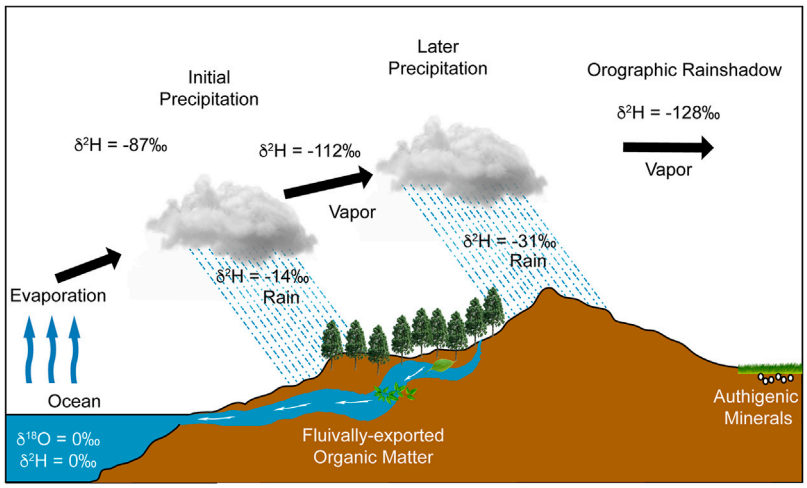

FIGURE 1 | Schematic of the "rainout" effect on precipitation (modified from Hoefs, 1997). Biomaker and organic matter export on the windward side and authigenic mineral formation and preservation within the a basin in the rainshadow.

proximity to the area of evolving topography (signal preservation).

In large accretionary collision zones, sediment is commonly preserved in foreland basin systems - elongate regions of sediment accommodation that form in response to geodynamic processes related to subduction (e.g., DeCelles and Giles, 1996). As orogens evolve, sediment deposition sites can vary from deep marine to fluvial and lacustrine deposition in a range of accommodation spaces. Thus, the sedimentary record of orogenesis spans a range of sediment composition and depositional settings. However, records of paleotopography frequently derive from only the terrestrial sediments associated with orogenesis. The most commonly utilized methodology for paleotopography reconstruction, stable isotope paleoaltimetry, is generally not applicable to marine sediments.

In many terrestrial continental environments such as the western North American interior, the Andes or Tibetan Plateau, prevailing wind directions and the orientation of the orogens produce large "orographic rainshadows" and a clear isotopic shift in precipitation that can be preserved in materials deposited within basin sediments close to the orogen. Conventional stable isotope paleoaltimetry generally assumes an airmass travels over an orogen, imparting a clear "elevation" signature on precipitation isotopes (**Figure 1**). Indeed, most paleoelevation studies utilize materials preserved in basin sediments within an orographic rainshadow. For example, virtually all records of the paleotopography of the Tibetan Plateau are generated from sediments deposited in basins now on the Plateau itself (Rowley et al., 2001; Molnar et al., 2006; Rowley and Currie, 2006; Rowley, 2006/8; Polissar et al., 2009; Xu et al., 2010; Quade et al., 2011; Staisch et al., 2014; Huntington et al., 2015; Currie et al., 2016; Tang et al., 2017; Li et al., 2019), with few studies from the Himalayan front (e.g., Hoke et al., 2014; Grujic et al., 2018).

While most paleotopography approaches require an orographic and isotopic rainshadow, in reality, variables such as atmospheric stability and wind-speed influence the path an airmass travels (e.g., Roe, 2005; Galewsky, 2009; Lechler and Galewsky, 2013). As orogens reach critical elevations, airmasses can travel laterally along a barrier rather than over, producing heterogeneous patterns of isotopes of precipitation in the leeward side of a range (Roe, 2005; Galewsky, 2009; Lechler and Galewsky, 2013; Wheeler et al., 2016). Similarly, changes to thermal heating of the landscape can alter moisture transport and isotope fractionation patterns (Poulsen et al., 2010; Insel et al., 2012; Insel et al., 2013; Botsyun et al., 2019). This can produce highly spatially heterogeneous geochemical signatures of topography. As a result, uplift of an orogen may not always produce clear isotopic signatures of elevation within an orographic rainshadow (e.g., Hren et al., 2009; Insel et al., 2010; Insel et al., 2012; Feng et al., 2013; Insel et al., 2013; Botsyun et al., 2016; Botsyun et al., 2019; Shen and Poulsen, 2019). A prime example of this process is observed in the Himalaya and Tibetan Plateau. Here, water isotope records show a large precipitation isotope gradient on the front of the Himalayan orogen, yet large-scale enrichment of water isotope values with progressive distance into the continental interior (Garzione et al., 2000; Hren et al., 2009; Jay; Quade et al., 2011; Bershaw et al., 2012; Yang et al., 2012; Yang et al., 2012). The isotopic shift that results from progressive mixing of multiple moisture sources combined with increased evaporation in the high elevation, arid landscape of the Tibetan plateau, can dwarf the isotopic signature that is related to elevation and observed on the range front or in close proximity to the orogen.

In contrast to the complex isotopic patterns observed in the leeward side of large orogens, particularly with increasing distance from an orographic barrier, along the range front of virtually all orogens on the globe, isotopes of precipitation generally show a clear and consistent relationship between elevation and water $\delta^{18}O$ or $\delta^{2}H$ and temperature. This geochemical signature can exhibit greater noise at lower elevations (less than 1 km) where local climatic and

atmospheric conditions can dominate (e.g., blocking and temperature inversions). However, over larger topographic ranges (several km) this pattern of temperature and precipitation isotope change in relation to elevation is fairly consistent. This pattern is true in the windward face of the Sierra Nevada (Ingraham and Taylor, 1991), Cascades (Hren, Unpublished), Himalaya (e.g., Garzione et al., 2000; Hren et al., 2009; Li and Garzione, 2017), northern and southern Andes on both east and west sides (Gonfiantini et al., 2001; Stern and Blisniuk, 2002; Smith and Evans, 2007; Saylor et al., 2009; Hoke et al., 2013; Valdivielso et al., 2020), the Alps (Giustini et al., 2016), Southern Alps (Poage and Chamberlain, 2001), topical mountain systems such as the Sierra Oriental of Mexico (Quezadas et al., 2015) and Taiwan (This study), tropical regions within Africa and South America (Gonfiantini et al., 2001), even isolated peaks such as Mauna Loa, Hawaii (Scholl et al., 1996; Scholl et al., 2007) and Mount Kilimanjaro (Zech et al., 2015). In fact, the pattern of precipitation isotopes and temperature as a function of elevation is far simpler to predict for the windward side of an orogen, where the majority of water vapor is removed from an airmass during orographic lifting and cooling, than for the leeward side, where atmospheric oscillations, high degrees of evaporation and mixing of multiple moisture sources can produce complex and spatially heterogeneous water isotope patterns. This observation highlights the need for new paleotopography approaches that take advantage of climatic and isotopic patterns observed on the windward side of an orogen, as well as materials that are preserved in marine deposition sites.

Organic Molecular Biomarkers and Paleoelevation

Terrestrial plants produce a variety of compounds within and on their leaves to minimize water loss and provide protection from predation (Holloway, 1969; Barthlott and Neinhuis, 1997). These molecules are produced in abundance and can be preserved over long timescales with minimal or no isotopic alteration (Schimmelmann et al., 1999; Schimmelmann et al., 2006; Yang and Huang, 2003/3). Plants utilize ambient water during biosynthesis and incorporate the isotopic signature of that water into biomolecules. The chemistry of these molecular compounds records water isotopes modified by factors such as evapotranspiration and carbon assimilation rates (e.g., Ehleringer et al., 1990; Chikaraishi and Naraoka, 2003/6; Chikaraishi et al., 2004; Sachse et al., 2004; Sachse et al., 2004; Sachse et al., 2006; Hou et al., 2008; Sachse et al., 2012). Compound-specific D/H fractionation in plant molecules is primarily dependent on water isotope composition, the biosynthetic pathway (Hayes, 1993) and stomatal water loss in response to water and CO_2 limitation, but integrated soil biomarkers commonly show consistent D/H fractionation in warm/temperate and moist environments (e.g., Sachse et al., 2012; Tipple and Pagani, 2013; Wang et al., 2017). In temperate and tropical environments, soil *n*-alkane δ^2H is correlated with precipitation δ^2H due to ecosystem level homogeneities of the vegetation (e.g. Jia et al., 2008; Tipple and Pagani, 2013; Tipple and Pagani 2013; Bai et al., 2015; Zhuang et al., 2015; Liu et al., 2016; Vogts et al., 2016; Bai et al., 2017; Wang et al., 2017; Liu and An 2019). For example, a study of precipitation isotopes and plant wax δ^2H along an elevation gradient of nearly 4 km on the SE margin of the Tibetan plateau shows a strong correlation between ambient water isotopes and *n*-alkane δ^2H over a range of elevations (Wang et al., 2017). In addition, the magnitude of change in *n*-alkane δ^2H observed on the SE Tibetan Plateau margin mirrors that observed in other regional studies from the SE Asian region (Jia et al., 2008; Bai et al., 2015). Some studies suggest that the relationship between plant wax δ^2H and ambient water may vary as a function of climate and/or elevation in some circumstances, however this remains a subject of debate with recent studies showing no climatic effect on apparent fractionation (Struck et al., 2020), and is similar to questions surrounding uncertainties in water of formation for authigenic minerals and glasses that are commonly used for paleoelevation reconstruction. Plant waxes, including long-carbon chain normal alkanes, can thus provide a geochemical record of ambient water δ^2H with similar or less uncertainty than other commonly used paleoprecipitation isotope proxies such as soil carbonates, clays, or volcanic glass. In addition, the molecules that are produced by plants and some terrestrial microorganisms, can be uniquely identifiable from molecules produced by marine organisms, meaning they can be identified and isolated from marine sediments.

Organic molecular biomarkers are produced by plants and microorganisms over nearly the entire range of global climatic conditions (with the exception of extreme cold environments) and can be preserved in nearly all sedimentary sinks associated with orogenesis. As a result, organic molecular biomarkers are increasingly utilized for paleoclimate/paleohydrology and paleotopography reconstruction (e.g., Polissar et al., 2009; Hren et al., 2010; Aichner et al., 2015; Hepp et al., 2015; Tuthorn et al., 2015; Rohrmann et al., 2016; Schafer et al., 2018; Bliedtner et al., 2020). These molecules can record two specific parameters that are commonly linked to elevation, present and past: 1) the stable isotopic composition of environmental water, and 2) the temperature at which molecules are synthesized. These two variables are related to processes associated with changes to ambient conditions and elevation such as Rayleigh distillation of water vapor during orographic lifting or adiabatic cooling of ambient air as a function of elevation. What is unique about organic molecular biomarkers in comparison to other records of environmental conditions, water isotopes and topography, is that these biomarkers can be produced and preserved on the windward and leeward sides of an orogen and are actually produced in greater abundance in warm and wet environments. As an archive of terrestrial environments, these materials provide a potential record of geochemical conditions on land, independent of whether or not they are preserved in a terrestrial or marine setting.

Organic Molecular Hypsometry: Catchment Integration of Water and Sediment

The $\delta^{18}O$ and δ^2H of stream waters record the precipitation and precipitation isotope-weighted hypsometry of the upstream catchment (e.g., Hren et al., 2009; Rowley et al., 2001; Rowley

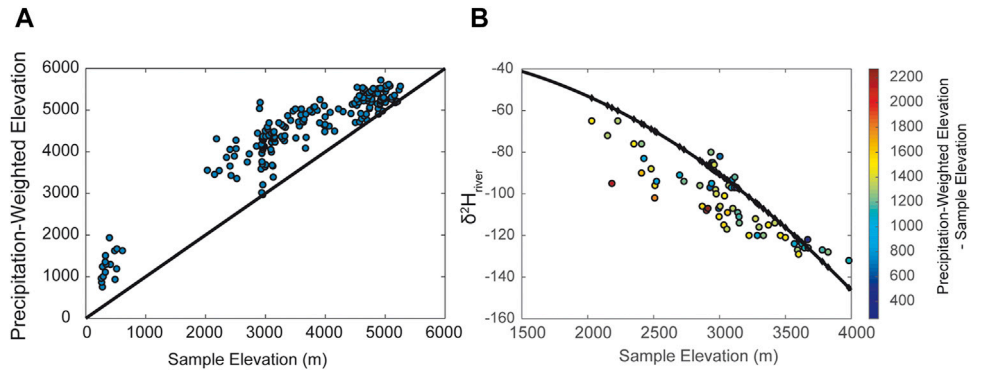

FIGURE 2 | (A) Comparision of sample elevation vs. precipitation weighted elevation for catchments from southern Tibet along the Brahmaputra and tributaries. **(B)** Sample elevation vs. hydeogen isotopes of stream waters from Southern Tibet relative to predicted water isotope δ^2H using a simple model of Rayleigh distillation after Rowley and Peirrehumbert 2001 (Data and predicted δ^2H taken from Hren et al., 2009). Shading of individuals points reflects the difference between the elevation at the location of the river water sample, and the upstream precipitation–weighted elevation for the point. Large deviations between measure δ^2H and pressure δ^2H generally result from significant differences between precipitation–weighted elevation and local sample elevation. Large offsets equal greater water contributions from higher elevations.

and Garzione, 2007). For example, along the Himalayan front, the $\delta^{18}O$ or δ^2H of river water from low sample elevations reflects isotopically depleted values that are consistent with precipitation-weighted elevation (Hren et al., 2009). Thus, the isotopic signature of water at any point on a river will generally reflect the isotopic composition of the precipitation-weighted elevation of the upstream area (**Figure 2**). Conceptually, this principle is quite simple and river water isotope signatures should reflect the distribution of water isotopes throughout the catchment weighted by the contributions from different portions of the basin. Indeed, more than 25 years ago, Norris and others (1996) argued that isotopic records of the Eocene Green River lakes provided clear indication of a high elevation paleo-Uinta Mountain range (Norris et al., 1996).

Annual precipitation δ^2H typically varies by ~15–30‰ per km of elevation in tropical to temperate settings (e.g., Poage and Chamberlain, 2001). The relationship between precipitation isotopes and elevation is most consistent in close proximity to an orogen and tends to increase in noise when the scale of the study area exceeds the scale of the processes that generate the geochemical signal. In large catchments, the isotopic composition of precipitation can vary by more than 100‰ in δ^2H from headwaters to river mouth (**Figure 2**), and the isotopic composition of water at any point along the river (which integrates the entire upstream area) can be quite distinct from the composition of precipitation falling on that point of the landscape. As one moves up a river profile, local elevation increases and catchment size decreases, and the offset between the local elevation of a point on a river and the mean elevation of the upstream area decreases to zero (**Figure 2**). As these come closer together, precipitation-weighted δ^2H becomes identical to ambient precipitation δ^2H.

Like water, fluvially-transported organic biomarkers can record the hypsometry of a catchment through their isotopic composition (where $\delta^2H_{biomarker}$ varies in relation to elevation-dependent variations in source water δ^2H) or in molecules that reflect the temperature of formation at a specific location in the catchment. To first order, plant waxes record the hydrogen isotope composition of water used during growth and show a similar $\Delta\delta^2H_{n\text{-alkane}}$ with elevation as precipitation (e.g., Jia et al., 2008; Bai et al., 2015; Zhuang et al., 2015; Nieto-Moreno et al., 2016; Wang et al., 2017). There are a number of factors that can influence the apparent fractionation between plant waxes and ambient water, including plant-specific differences in evapotranspiration and biosynthesis (e.g., Sachse et al., 2012), and some data suggests potential changes in apparent fractionation with elevation (Bai et al., 2017). However, other data suggests no clear correlation between climate and apparent fractionation (Struck et al., 2020) and numerous studies of biomarkers in soils show a generally consistent fractionation between water and wax (Jia et al., 2008; Tipple and Pagani 2013; Bai et al., 2015; Zhuang et al., 2015; Liu et al., 2016; Vogts et al., 2016; Bai et al., 2017; Wang et al., 2017; Liu and An 2019). Here we present new organic molecular biomarker and water isotope data from soils and rivers of Taiwan to test whether organic biomarker isotopes can reflect catchment integrated signatures of catchment hypsometry.

Taiwan: A Model System for Studying Catchment Integration and Biomarker Records

The island of Taiwan marks the active boundary of the Eurasian and Philippine Sea plates (Teng, 1990) and hosts some of the highest rates of convergence, exhumation (Yu and Chow, 1997; Dadson et al., 2003; Lee et al., 2015), erosion (Hovius et al., 2000; Dadson et al., 2003; Schaller et al., 2005; Siame et al., 2011/4; Derrieux et al., 2014), and precipitation on the globe. The nearly 400 km long orogenic belt is a product of the oblique collision of the north-trending Luzon Arc and the northeast-trending passive margin of southeast China and is commonly used as a model for an active accretionary wedge (Ho, 1986; Y.-H.; Lee et al., 2006;

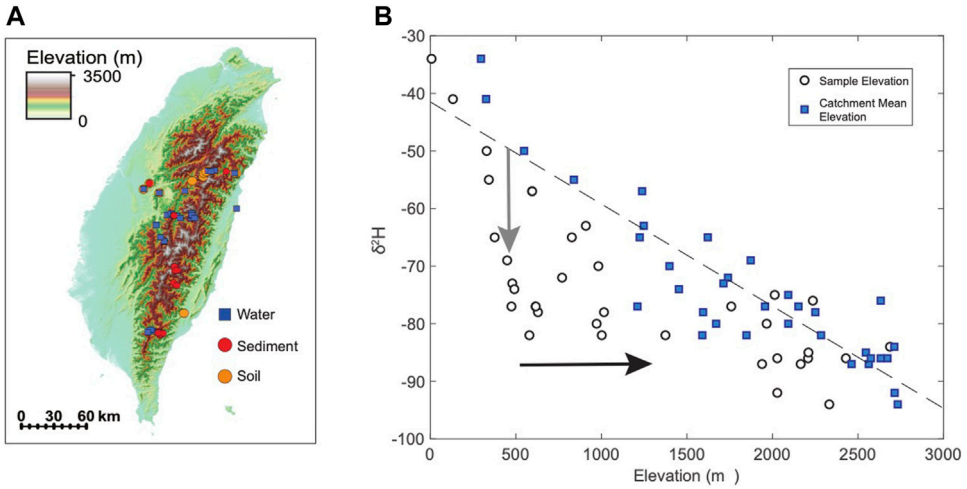

FIGURE 3 | (A) Sample location of water, soil, and sediment samples used in this study. **(B)** δ^2H of river waters (plotted as sample elevation and as catchments mean elevation). Gray arrow represents the deviation between the δ^2H of waters at a sample elevation and the expected δ^2H of local precipitation. Black arrow shows the deviation between the elevation of a sample vs. the elevation of the contributing watershed.

Teng, 1990). Taiwan is also provided as an example of an orogenic system that is in a topographic steady state (Suppe et al., 1981; Willett and Brandon, 2002; Stolar et al., 2007), where the flux of material to the base and front are balanced by the removal of material through physical and chemical erosion (Suppe et al., 1981; Deffontaines et al., 1994; Willett and Brandon, 2002). As a potential steady state orogen, Taiwan serves as an example for understanding the links and feedbacks among tectonics, climate, and erosion (Roe et al., 2006). However, to date, there is no known methodology to constrain the elevation history of orogens such as Taiwan due to the lack of an orographic rainshadow, extremely rapid erosion with minimal onshore terrestrial sediment storage, and the lack of datable carbonates, clays or glasses that could preserve a record of isotopic change due to uplift. As such, it is an ideal location to test a new approach to constraining paleotopographic change.

Taiwan does not have an orographic rainshadow (with high precipitation and moisture sourced from both the east and west), however it is characterized by large temperature and precipitation isotope gradients with elevation. We sampled thirty-three stream waters (**Table 1**) and twelve modern soils (**Table 2**) across Taiwan from 0 to 3,500 m to examine the modern relationship between $\delta^2H_{n\text{-alkane}}$, elevation, and precipitation δ^2H (**Figure 3**). In addition, we collected sixteen river sediments (**Table 3**) at sites adjacent to soil collection localities to assess catchment integration signatures within the organic molecular biomarker pool. Soils were collected from locations in close proximity to the river channel, but well above any modern floodplain to avoid contributions from the modern river, and therefore are assumed to reflect only "local" biomarker production for this study. Fluvial sediments were collected from within the channel in an attempt to capture an integrated sediment signature. For each water and river sediment sample, we used ArcGIS to quantify the histogram of the contributing catchment and key parameters such as max/min/mean catchment elevation. Thus, water and sediment samples are characterized by both a "local" and "catchment mean" elevation that reflects the elevation the samples were collected at and the mean elevation of all areas potentially contributing to the sample collection point. Soil samples are considered "local" and may only be represented as a single sample elevation for the purposes of this work.

For biomarker extraction and analysis, samples were freeze-dried and approximately 150 g of sediment extracted via Soxhlet apparatus using a 400 ml mixture of dichloromethane:methanol (2:1, v:v). Organics were separated by polarity using silica gel column chromatography with hexane, methylene chloride and methanol. The nonpolar hexane fraction (S1) containing *n*-alkanes were further purified by urea adduction and silver nitrate ($AgNO_3$) chromatography to separate branched and cyclic alkanes. The distribution of normal alkanes was quantified using a Thermo-Scientific Trace GC Ultra equipped with a flame ionization detector (FID-GC-FID), using a BP-5 column (30 m × 0.25 mm i.d., 0.25 μm film thickness) with helium as the carrier gas at a constant flow rate of 1.5 ml/min. *n*-alkane δ^2H was analyzed for peaks of sufficient abundance using a GC-Isolink coupled to a Thermo- Scientific MAT 253 isotope ratio mass spectrometer (IRMS) using a BP-5 column (30 m × 0.25 mm i.d., 0.25 μm film thickness). The temperature program was set at 50°C for 1 min, ramped to 180°C at 12°C/min, then ramped to 320°C at 4°C/min and held isothermally for 4 min. During the interval of measurement, standards were analyzed every 4-5 four samples across a range of concentrations to correct for size and scale effects. Repeat analyses throughout the run and for a range of standard concentrations yield an external precision of <5‰ for δ^2H. All values are expressed in standard delta notation relative to VSMOW. The δ^2H of waters was analyzed by the Stable Isotope Laboratory at Louisiana State University and reported relative to VSMOW. Precision is <2‰ for δ^2H.

Water samples span the drainage divide and annual precipitation exceeds several m/yr over the study area. All areas

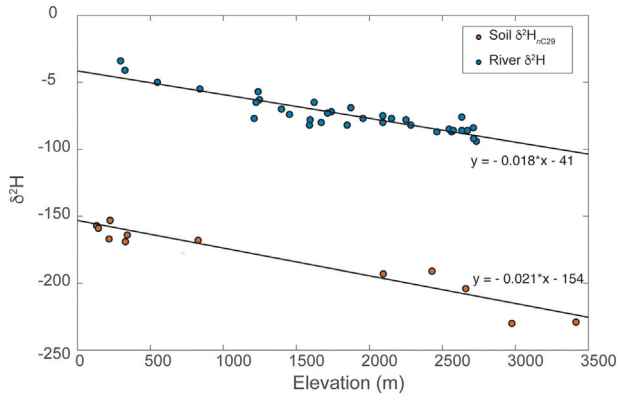

FIGURE 4 | Comparison of river water (mean upstream elevation) vs. δ^2H and soil site elevation vs. *n*-alkane δ^2H_{nC29}.

are also subject to extreme convection events, different seasonal monsoonal precipitation and typhoons. Given the high relief present in the Taiwan orogen, there is significant contribution from high elevation upstream areas to any given point in the river network. Given the extreme climate variability in Taiwan, one might predict that relationships between isotopes of precipitation and elevation would be highly variable between E and W sides and any elevation-dependent signatures could be muted by the large convective rainfall events. River waters represent a time-integrated groundwater signal. When river waters are plotted as a function of area-weighted elevation (the mean elevation of all portions of the catchment that contribute water to a specific sampling point on the river), the data reveal a classic elevation-dependent Rayleigh distillation pattern. Our data show that waters from the north to the south and collected over multiple years produce a well-defined isotope-elevation relationship (~18‰ per 1,000 m) (**Figures 3A,B**) when plotted as a function of catchment mean elevation. We suggest that river waters provide the best estimate of the time-integrated water isotopes incorporated into plants in Taiwan during biosynthesis. This is likely due to the fact that large rainfall events in Taiwan are associated with significant overland flow from the steep slopes of the high relief catchments. Thus, soil water and amount-weighted precipitation δ^2H may not be the same. Thus, we focus on river water isotope data which provide a clear expectation for an elevation-dependent isotopic signal within molecular biomarkers produced across the Taiwan landscape.

Soil-derived long-carbon chain *n*-alkanes show a similar pattern to water δ^2H, in support of our emphasis on river water data, and are suggestive of a consistent relationship between $\delta^2H_{n\text{-alkane}}$ and elevation (**Figure 4**). This pattern is not surprising, given the high degree of primary productivity at nearly all elevations across Taiwan and C3-dominated forests across nearly all elevations of the subtropical study area. The modern biomarker isotope lapse is on the order of ~21‰ for δ^2H_{nC29}, with a slightly lower lapse rate for nC_{31} and higher for nC_{27}. Thus, the isotopic lapse observed in plant biomarkers closely tracks that of river waters. This likely results from the subtropical climate, long-growing season, high precipitation, and angiosperm-dominated forests at all elevations. Thus, we can confidently argue that to first order, plant wax δ^2H records variations in the geochemical signature of precipitation that is a function of elevation and observed in countless other orogenic systems.

The isotope and molecular geochemistry of biomolecules produced throughout a catchment reflect the conditions at the location and time of biosynthesis. The pattern of precipitation isotopes that is observed within a catchment is thus reflected in the isotopic composition of organic biomarkers that are produced throughout that catchment. One might reasonably expect that organics produced at points throughout a catchment would reflect the pattern of water isotopes on the landscape in the form of an organic molecular isoscape. To illustrate this, we show the digital elevation map of the Mugua basin of eastern Taiwan (**Figure 5A**), with the expected biomarker δ^2H_{nC29} overlain as a colormap (**Figure 5B**). The "expected" biomarker δ^2H_{nC29} shown in **Figure 5B** is based on modern measured Taiwan soils from varied elevations (this study) using a simple linear isotope-elevation lapse for illustration purposes. At sea level, we assume a local soil δ^2H_{nC29} of ~-150‰ (equal to our most isotopically enriched, low elevation soil value), and a decrease of ~20‰ per kilometer of elevation, which lies between the measured lapse rate for river waters (18‰) and soils (~21‰).

As plants shed leaves and surface molecules are ablated throughout the catchment, molecular biomarkers can be integrated into soils and bound to clay minerals. Erosion of soils and downslope movement of biomass can then produce a mixed organic molecular isotope signature in river sediments that reflects the degree of integration of biomolecules sourced throughout the catchment (**Figure 5A**). Indeed, work in the Himalaya (e.g., Galy et al., 2011) and recent work in the Gaoping River system of Southeast Taiwan (Chang et al., 2021) shows evidence for downslope transport of organics and indicate that proximity to high relief, steep topography exerts considerable control over the degree of sediment and organic molecular integration in fluvial sediments. One of the great challenges of interpreting fluvial biomarker records is how sediments and organics integrate as they move from source to sink.

Taiwan catchments are generally steep and high relief, often spanning more than 3 km of elevation. Water samples collected at any point in a river reflect all the processes that occur upstream of the sample point. The high topography and steep Taiwan orogen means that the mean elevations of large Taiwan catchments are generally significantly higher (>1 km) than the elevation of the river mouth. Modern Taiwan river water data (this study) shows a significant offset between the isotopic composition of water sampled at a point in a river and the expected composition of precipitation isotopes that might fall at the elevation of the river water sample site (**Figure 3**). The offset between the expected δ^2H composition of precipitation for a given elevation and measured river water δ^2H at that elevation can be up to 30‰. This difference is greatest at low elevations, where the offset between the site elevation and the hypsometric mean elevation of the upstream area is largest.

Modern water δ^2H and soil-derived *n*-alkane δ^2H data can be used to predict the magnitude of isotopic offset that would result from catchment integration of sediments and molecular biomarkers. Data show that in a Taiwan catchment with

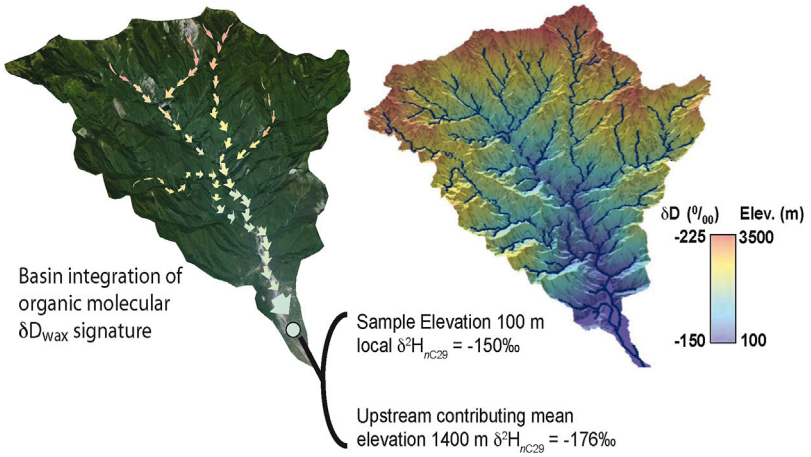

FIGURE 5 | (A) Schematic of basin integration of sediment and contributing molecular components. **(B)** Modeled δ^2H_{nC29} of plant–derived normal alkanes throughout the Mugua basin of eastern Taiwan. Plant wax δ^2H_{nC29} values reflect modern soil δ^2H_{nC29} data from samples acreoss Taiwan.

3.5 km of relief such as the Mugua basin (**Figure 5**), soil *n*-alkane δ^2H should vary from ~150‰ at low elevation to as negative as −225‰ at elevations in excess of 3 km (**Figures 4**, **5**). Erosion and basin integration of this material will bias the isotopic signature of sediments deposited in floodplains and low elevation sites. If the expected change in *n*-alkane δ^2H in plants and soils as a function of elevation is known (signal generation) and one can estimate the contribution of biomolecules from each point in the landscape (a molecular production and erosion function), it is possible to calculate the expected $\delta^2H_{n\text{-alkane}}$ of an integrated sedimentary flux. For example, based on modern Taiwan soil *n*-alkane δ^2H data from varied elevations, the δ^2H of *n*-alkanes deposited at the river mouth within a hypothetical catchment with relief of >3 km and a mean elevation of ~1.25 km, should be ~25‰ more negative than the ambient vegetation growing at that elevation (**Figures 5A,B**), if all areas of the catchment contribute equally to the biomarker flux and the catchment is characterized by a constant apparent fractionation between ambient water and biomarker δ^2H and no loss (oxidation) of *n*-alkanes during transit. In practice, the question is whether or not the organic molecular signal preserved in fluvial sediments is biased to specific elevations or portions of a catchment, much as lithology, relief and landslide frequency might bias cosmogenic isotope signatures of catchment average erosion rates in non-equilibrium landscapes (e.g., Willenbring et al., 2013).

To test this conceptual model of catchment integration of biomarkers, we measured the offset between modern soil-derived *n*-alkane δ^2H_{nC29} and those preserved in fluvial sediments at similar elevations along the river profile. The expectation is that for a given point along a river profile, local soils should show δ^2H_{nC29} values consistent with local elevation whereas samples collected from within the river system should reflect integration of materials sourced from both local and upstream areas. Our data show that the hydrogen isotope signature of *n*-alkanes preserved in modern river sediments are strongly controlled by the hypsometry of the source catchment (**Figure 6**). Specifically, we plot the δ^2H_{nC29} in soils adjacent to river systems as a function of their sample elevation. This is compared to the δ^2H_{nC29} in sediments within the river channel, which should reflect some degree of sediment/organic contributions from upstream contributing areas (**Figure 6A**). The hydrogen isotope signature of fluvially-transported *n*-alkanes sampled at low elevation deposition sites (i.e., floodplains) are commonly depleted by tens of per mil relative to low elevation soils (**Figure 6A**). At higher elevations within the catchment (areas of sediment generation rather than sediment sink), there is no observable offset between soil δ^2H_{nC29} (local signal) and sediment δ^2H_{nC29}. What this means is that not surprisingly, low elevation fluvial sediments preserve a geochemical signature of upstream contributions of organic matter and that this signature can be quite significant. The isotopic shift associated with this downslope transport of organic matter is shown by the grey arrow (**Figure 6A**) which indicates more negative fluvial sedimentary δ^2H_{nC29} relative to local soils at the same sample elevation. For example, river sediments collected at a local elevation of ~500 m may yield a δ^2H_{nC29} value of −180‰, which is 20‰ more negative than one might expect for local soils at that elevation. We can examine what the magnitude of the observed offset between soil and fluvial sediment δ^2H_{nC29} means by considering a scenario where all portions of the landscape contribute equally to the biomarker flux exported in river sediments. If the biomarker δ^2H data from river sediments are plotted as a function of contributing upstream hypsometry (area-weighted elevation), soil and river alkane δ^2H_{nC29} data reconcile and fall along the same profile. This qualitative agreement strongly suggests that exported sediments reflect the hypsometry of organic matter within the catchment and means that if all areas of the upstream catchment equally contribute to this river sediment, we might expect that the mean elevation the sedimentary organic matter is sourced from is actually 1–1.5 km higher than the elevation of the sample point along the river. Thus, the geochemical signal of river sediments records information about catchment integration and source elevation. For Taiwan, the δ^2H_{nC29} of fluvially-

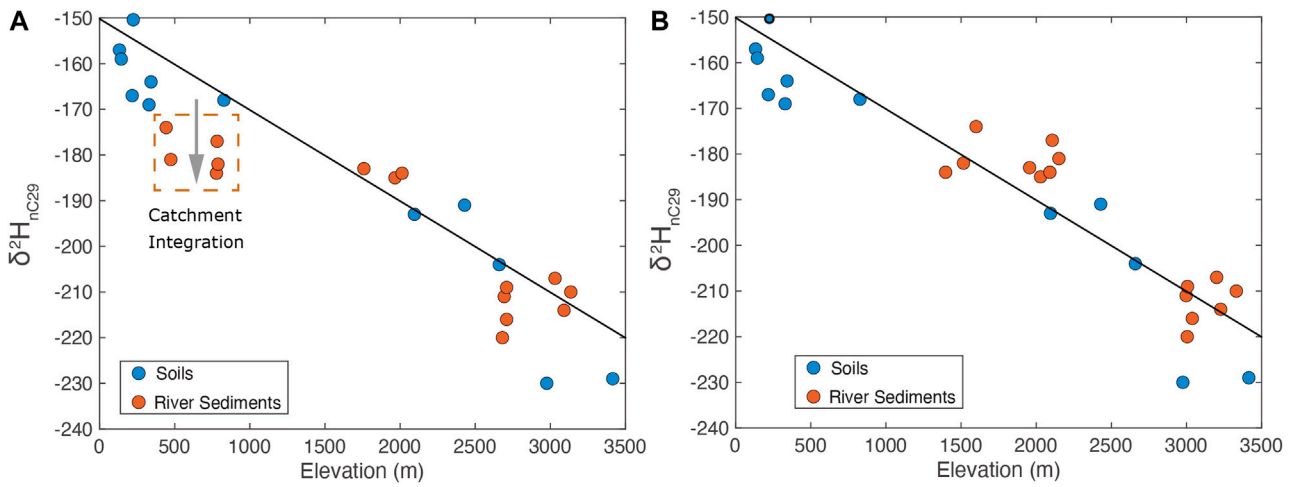

FIGURE 6 | (A) Soil δ^2H_{nC29} (blue circles) and ricer sediment δ^2H_{nC29} (orange circles) vs. sample elevation. Biomarkers produced throughout the Taiwan orogen generally mirror the pattern of δ^2H_{nC29} variation observed in ambient waters. The δ^2H_{nC29} of low elevation, fluvially–deposited alkanes are negative relative to the δ^2H_{nC29} from low elevation soils. The gray arrows shows the direction that downslope transport/catchment integration of biomarkers will shift the δ^2H_{nC29} fluvially–transported alkanes. The solid line represents soil δ^2H_{nC29} data as a function of elevation with a sea level value of –150‰ and a lapse rate of –20‰ per km. **(B)** Soil δ^2H_{nC29} vs. sample collection elevation (blue cicles) and river sediments δ^2H_{nC29} vs. the mean elevation for all areas of the catchment upstream of the river sediment sample location. Plotting river sediments δ^2H_{nC29} as a function of mean elevation of the area upstream of the sample collection elevation reconciles soil (local) and river sediment (integrated) data, demonstrating significant contributions biomarkers produced throughout the catchment to the site of sediment deposition.

transported organics is consistent with the integrated isotopic signature of organic matter produced throughout the catchment (i.e., δ^2H_{nC29} of organics produced at the catchment mean elevation).

In general, there is a solid basis for the expectation that fluvially-transported biomarkers might represent a catchment mean isotopic signature in Taiwan. First, river water isotopes show a clear isotope-elevation relationship when considered in the context of catchment integrated signals (area-weighted contributions). To first order, catchment integration of water should behave similarly to integration of other components of the system (sediment, organic matter). Second, Taiwan's subtropical/tropical climate results in a high degree of biomass production over nearly the entire elevation range of the orogen. All portions of Taiwan catchments contribute to biomarker production, though we recognize that climatic and biologic factors may impose variations in biomarker production rates with elevation. Third, the Taiwan landscape is characterized by extremely high rates of exhumation and erosion (associated with the frequent earthquakes, numerous annual typhoons, and high precipitation rates) and rapid turnover of the soil carbon pool. Hilton et al. (2008) suggests that up to 77% of non-fossil carbon may be exported via large events on the decadal timescale and ^{14}C ages of fluvial biomarkers in Taiwan rivers yield ages on the order of hundreds of years old (Eglington et al., 2021). Rapid export of organics is readily replaced by new vegetation due to the high temperature and abundant precipitation over nearly all elevations within the tropical setting. Thus, there is relatively short carbon residence time in soils and sediments within the Taiwan orogen. Fourth, *n*-alkane δ^2H are not significantly affected by degradation effects that may occur during transport or storage (Zech et al., 2011; Brittingham et al., 2017).

One consideration when measuring biomarker integration signatures is the potential contribution of legacy carbon that can bias the contributions of fluvially-exported leaf waxes. In Taiwan, much of the exposed and rapidly eroding sediments present in the orogen have undergone metamorphism at temperatures in excess of several hundred degrees. This heating results in a breakdown of long-carbon chain normal alkanes that tends to degrade many of the compounds analyzed for organic molecular reconstructions. As a result, legacy carbon is not a significant complication in a setting such as this. Indeed, modern bedrock samples from the slate belt of Taiwan show minimal to no long-carbon chain *n*-alkanes that would potentially bias the modern isotopic signature of organic molecules. This is not the case in all locations of the western foreland, where Plio-Pleistocene sediments are being uplifted and eroded and contain measurable long-chain normal alkanes. However, ancient sediments there are generally characterized by low abundances of target biomarkers, so while they are likely to be a potential contaminant of concern, legacy contributions are minor compared to active input from primary production in the warm and wet tropical climate.

Applying Organic Molecular Paleohypsometry

In recent years, multiple studies have observed downstream transport of organic biomarkers sourced from higher elevations. This includes both plant-derived biomolecules such as *n*-alkanes and fatty acids, as well as soil-derived compounds commonly utilized to reconstruct past temperature. (e.g., Galy et al., 2011; Ponton et al., 2014; Feakins et al., 2016; Hoffmann et al., 2016; Feakins et al., 2018; Usman et al., 2018; Zhuang et al.,

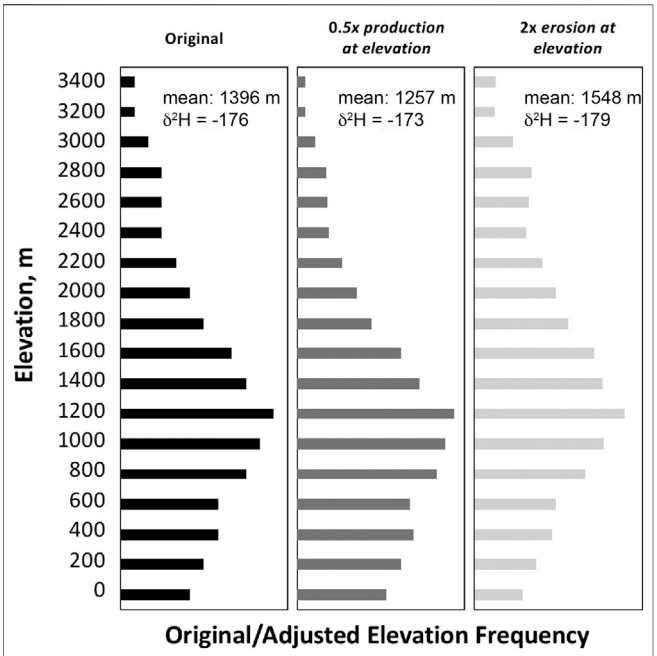

FIGURE 7 | Modeled biomarker–weighted area/elevation distribution for three scenarios of biomass production and erosion as a fuction of elevation. These include **(A)** constant production and erosion as a function of elevation, **(B)** a halving of biomass production from 0 to 3000 m, and **(C)** a doubling of erosion as a function from 0 to 3000 m. Each scenario assumes a constant isotopic lapse rate.

2019; Kirkels et al., 2020). Studies from a range of landscapes show downslope transport of biomarkers can bias geochemical signatures preserved in low elevation sites yet interpreting these data may be complicated. For example, storm and mass wasting events are shown to produce greater mobilization of materials from the steep proportions of a catchment (Wang et al., 2020). While organic molecular paleohypsometry has the potential to provide a means of quantifying changes in the elevation distribution of biomass within an orogen, reliable application of such an approach to ancient sediments requires constraints on several variables. In particular, how does catchment geometry and climate influence the degree of contribution of biomass from across a catchment? Is the contribution of biomolecules uniform or weighted to specific elevation ranges within a catchment? In the Taiwan example shown above, we used the assumption that all areas of the landscape contributed equally to the biomolecule flux. Is this a reasonable assumption? How do changes to climate that are associated with the evolution of an orogen influence the contribution of biomarkers from different portions of a catchment?

Application of an organic molecular paleohypsometry approach requires a number of assumptions to relate measured *n*-alkane δ^2H to catchment/molecular hypsometry. To examine how sensitive resultant paleohypsometry interpretations are to assumptions for molecular production and integration, we modeled three scenarios of biomarker production, erosion and integration for a hypothetical catchment (**Figure 7**; Supplemental file). We use a synthetic catchment histogram (area-elevation distribution) and chose three elevation-dependent functions for production and sediment erosion, and display these in elevation frequency plots (**Figure 7**), where the bar length is proportional to the area-elevation contribution within the hypothetical catchment. The goal of this sensitivity test is to ask the question, how do elevation-dependent differences in the production or erosion of molecular biomarkers affect the integrated signature of materials mobilized through a catchment and deposited in the river mouth. These tests include an assumption of 1) constant biomarker production and sediment erosion at all elevations within a catchment; 2) A decrease in biomarker production by 50% from sea level to 3,000 m and constant sediment erosion for all elevations in the catchment; and 3) constant biomarker production at all elevations in the tropical catchment but a doubling of erosion rates/contribution as a function of elevation from 0 to 3,000 m. These scenarios represent some of the endmember conditions that shape the isotopic signature of catchment integration but are based on observed patterns of organic biomass production or sediment erosion observed in the real world. We include two additional scenarios (shown in **Supplementary Scenario**) where 4) organic production decreases exponentially as a function of elevation by 75% from 0 to 2000 m and almost 90% by 3,000 m and 5) erosion increases exponentially as a function of elevation with more than 8 times the erosion rate at 3,000 m as at sea level, and biomass production decreases by 50% from 0 to 3,000 m.

Differences in production or erosion as a function of elevation will produce a difference in the area-weighted elevation of source materials (biomarkers). For example, if biomarkers are produced and eroded evenly throughout a catchment, mass balance dictates that the mean source elevation of biomarkers exported to the river mouth is equal to the catchment mean elevation. For a constant isotope-elevation lapse rate, the δ^2H of exported biomarkers is therefore equal to the δ^2H of biomarkers produced at the mean elevation. Factors that bias the production or erosion of biomarkers to higher or lower elevations in a catchment would then shift the mean biomarker source elevation higher or lower. To test how different assumptions for biomarker production and sediment erosion as a function of elevation might affect the δ^2H_{nC29} of river sediments and biomarkers transported through the river system and deposited at a river mouth (reflecting the integrated signature of production and erosion throughout a catchment), we use modern Taiwan soil δ^2H_{nC29} data and assume that soils formed at sea level are characterized by a δ^2H_{nC29} of −150‰, and those formed at elevation are modified by a biomarker δ^2H_{nC29} lapse of 20‰ per km elevation in the catchment, similar to the pattern observed in surface waters.

For the different endmember conditions of production/erosion we modeled, there is a distinct pattern of biomarker contribution from different elevations to the overall riverine flux. These produce distinct histograms (**Supplementary Scenarios S1–3** shown in **Figure 7**) with the bar length representing the overall biomarker contribution to the fluvial load from each elevation bin. Each of these scenarios uses the same elevation histogram (the same catchment) but produces distinct mean-

biomass contribution elevations (the abundance-weighted elevation of all organic matter contributing to the fluvial signal at the river mouth) and biomarker δ^2H_{nC29} associated with that mean-biomass value. The calculated δ^2H_{nC29} of each scenario can be thought of as the isotopic composition that one would expect to measure in sediments collected at the river mouth for the hypothetical catchment with the associated production/erosion functions. What this shows is that differences in production/erosion of biomarkers over the range of elevations in a catchment can bias the exported geochemical signal to higher or lower portions of a catchment. Yet, for each of the three different production/erosion functions, the calculated δ^2H_{nC29} values for the sediments deposited at the river mouth are relatively consistent, ranging from −173 to −179 (**Figure 7**). In the context of isotope-elevation lapse rates, this translates to ~300 m elevation difference. What this sensitivity test means is that for these three scenarios of varied molecular production and erosion as a function of elevation, we might expect that fluvial sedimentary biomarkers deposited at the river mouth are 23–29‰ more negative in δ^2H than soils formed in the ambient environment at the sediment deposition site, with mean organic matter contribution elevations of 1,257–1,548 m for the three scenarios. These values closely align with the true area-weighted mean elevation of the catchment of 1,396 m. Thus, regardless of our assumptions of the production/erosion function, the measured δ^2H_{nC29} value of organics sampled at the river mouth closely approximate the δ^2H_{nC29} value of organics one would predict to form at and represent the catchment mean elevation. This quantitative examination is generally consistent with the qualitative agreement shown in **Figure 6B**.

Sensitivity test results suggest that in the context of evolving topography through time, a range of changes to primary production or erosion over time could occur without dramatically influencing the overall relationship between catchment hypsometry and exported isotope signature. If true, then sedimentary records of biomarker δ^2H_{nC29} could reliably record changes in catchment hypsometry through time, even though there remain considerable uncertainties in molecular production and erosion. We caution however, that other changes such as factors that could produce a bimodal distribution of biomarker export as a function of elevation, or climatic effects that result in significant decrease in organic production with elevation, could in fact exert significant changes to the magnitude of offset between the elevation of sediment deposition site, and the elevation predicted based on fluvial biomarker δ^2H_{nC29}. For example, if organic biomarker production decreased by 50% from sea level to 1 km and by 75% at 2 km elevation (**Supplementary Scenarios S4**), the mean source elevation of fluvial sediments sampled at sea level would be 1,004 m, ~400 m below the true catchment mean elevation. Sediments sampled here would be expected to have a δ^2H_{nC29} of ~ −168‰. Such a scenario is not realistic for a setting such as Taiwan as data from tropical settings indicates a decrease in primary productivity on the order of 50% between 0 and 3,000 m elevation (e.g., Mahli et al., 2017). Likewise, if erosion increased exponentially with elevation and organic production decreased by 50% from 0 to 3,000 m (**Supplementary Scenarios S5**), the mean source elevation of organics would be 1720 m and sediments sampled at the river mouth would be expected to have a δ^2H_{nC29} of ~ −182‰. This scenario produces a source elevation ~300 m higher than the catchment mean. These examples illustrate how differences in production or erosion could bias to the elevation distribution and isotopic composition of contributing organics. Importantly however, all scenarios produce values within several hundred meters of the catchment mean elevation.

New data from Taiwan demonstrates the potential utility of fluvially-exported molecular biomarker isotopes to quantify the hypsometry of a catchment and we provide qualitative and quantitative arguments to suggest these data are consistent with a catchment mean elevation signature in a rapidly eroding tropical landscape. However, as a tool for long-term topographic reconstruction, organic molecular paleohypsometry faces similar constraints to the application of cosmogenic isotopes to quantify catchment average erosion rates (after Dosseto and Schaller, 2016). Specifically, what is the molecular production function? Is there temporal variability in the storage in the weathering profile? How does hillslope transport change over time? What are the timescales of river transport and temporary storage in river alluvium? Further refinement of this approach requires greater examination of the above and other factors. Here we provide a summary of several key steps in utilizing a molecular paleohypsometry approach to constrain changes to topography through time or the development of catchment relief.

(1) Molecular production function: The first consideration for application of a molecular paleohypsometry approach is the determination of a molecular production function. For each pixel of a catchment, how many molecules of the biomarker of interest are produced? Is this function uniform, is it biased as a function of elevation? How does climate influence this function? We show one potential example of a molecular production function in **Figures 5A,B** that is based on the modern soil δ^2H_{nC29} and assumes even production throughout the catchment. In reality, primary productivity of terrestrial biomass is generally a function of temperature and water availability (Amthor and Baldocchi, 2001). Studies from tropical forests of Peru show a nearly halving of gross and net primary productivity from sea level to 3,000 m elevation (Malhi et al., 2017). The decrease in primary productivity with elevation could lead to a biomarker production function that is nonlinear with elevation. Strong primary productivity differences could result in substantially greater molecular inputs at lower elevations relative to higher elevation sites. This scenario is obvious for locations with a treeline–above this elevation, molecular inputs would effectively be zero. Likewise, because primary productivity is known to scale with temperature and precipitation, the production function for specific biomolecules may vary as a function of current or paleo climatic conditions.

(2) Decay function: What is the rate of molecular degradation and is there a relationship to transit time? Malhi et al. (2017) show a halving of primary production over a 3 km gradient but also a general increase in carbon residence time with elevation, with longer residence time in higher elevation,

TABLE 1 | River water samples and basin parameters.

Name	Sample Date	δ^2H(water)	Longitude (dec. deg.)	Latitude (dec. deg.)	DEM Elevation	Drainage Area (km^2)	Basin Elevation			
							Elevation Mean (m)	Elevation Minimum (m)	Elevation Maximum (m)	Basin Relief (m)
OT13-01	2013	–65	120.951	23.789	376	16.7	1622	376	2862	2486
OT13-02	2013	–57	120.987	23.801	595	2.2	1238	595	1903	1308
OT13-03	2013	–77	121.014	23.785	474	689.7	2152	467	3822	3355
OT13-04	2013	–69	121.012	23.787	449	794.3	1873	449	3561	3112
OT13-05	2013	–78	120.925	23.549	1015	50.3	2250	1015	3926	2911
OT13-06	2013	–82	120.926	23.551	1002	33.3	2284	1002	3847	2845
OT13-07	2013	–72	120.891	23.587	770	91.0	1740	770	2858	2088
OT13-08	2013	–73	120.850	23.697	479	366.2	1713	479	3926	3447
OT13-09	2013	–63	121.041	23.782	909	0.4	1247	909	1519	610
OT13-10	2013	–82	121.073	23.761	1374	0.9	1848	1374	2264	890
OT13-11	2013	–87	121.174	23.764	2165	0.9	2462	2165	2785	620
OT13-12	2013	–76	121.179	23.785	2236	3.3	2633	2236	2782	546
OT13-13	2013	–86	121.185	23.796	2208	5.3	2633	2208	2928	720
OT13-14	2013	–87	121.177	23.807	1939	38.2	2563	1937	3258	1321
OT13-15	2013	–85	121.182	23.790	2210	0.5	2546	2258	2678	420
OT13-19	2013	–84	121.204	23.765	2687	0.1	2712	2676	2757	81
OT14-02	2014	–82	120.806	22.753	579	115.7	1590	579	2429	1850
OT14-03	2014	–78	120.817	22.759	629	39.5	1594	629	2219	1590
OT14-04	2014	–80	120.836	22.747	972	20.4	1670	972	2219	1247
OT14-05	2014	–70	120.837	22.746	982	2.3	1398	982	1730	748
OT14-07a	2014	–80	120.883	22.731	1966	0.7	2092	1966	2179	213
OT14-08	2014	–75	120.886	22.737	2013	1.7	2092	2012	2202	190
OT14-09	2014	–77	120.900	22.714	1759	2.1	1956	1752	2159	407
OT14-19	2014	–77	120.815	22.756	616	1.3	1211	616	1695	1079
OT14-20	2014	–74	120.789	22.737	491	8.7	1453	491	2703	2212
OT-15-1	2015	–41	120.727	24.016	132	3.0	326	143	744	601
OT-15-2	2015	–50	120.874	23.984	329	3.2	548	320	777	457
OT-15-3	2015	–65	121.111	24.006	827	3.4	1224	858	1568	710
OT-15-7	2015	–86	121.326	24.186	2429	0.3	2672	2448	2810	362
OT-15-9	2015	–94	121.353	24.184	2332	0.4	2732	2326	3001	675

(Continued on following page)

TABLE 1 | (*Continued*) River water samples and basin parameters.

Name	Sample Date	δ^2H(water)	Longitude (dec. deg.)	Latitude (dec. deg.)	DEM Elevation	Drainage Area (km^2)	Basin Elevation			
							Elevation Mean (m)	Elevation Minimum (m)	Elevation Maximum (m)	Basin Relief (m)
OT-15-10A	2015	–86	121.385	24.193	2028	1.5	2575	2016	3052	1036
OT-15-10B	2015	–92	121.385	24.193	2028	5.3	2714	2025	3336	1311
OT-15-11	2015	–55	121.571	24.169	342	0.4	839	359	1315	956
OT-15-12	2015	–34	121.594	23.853	7	6.9	296	19	585	566

TABLE 2 | Modern soil samples and *n*-alkane hydrogen isotopes.

Sample	Latitude	Longitude	Sample Elevation	n	δ^2H_{nC27}	δ^2H_{nC29}	δ^2H_{nC31}	$\delta^2H_{nC27-31}$	ACL
OT-15-1	24.016	120.727	132	2	–145	–157	–167	–157	28.5
19TW-LW19 A	24.171	121.590	144	2	–158	–159	–162	–176	-
OT-15-13	22.913	121.119	217	2	–167	–167	–162	–165	30.0
MT-TW-07b	120.781	24.069	224	1	–145	–150	–154	–151	-
OT-15-2	23.984	120.874	329	2	–167	–169	–162	–164	29.4
OT-15-11	24.169	121.571	342	4	–169	–164	–161	–162	30.5
OT-15-3	24.006	121.111	827	2	–171	–168	–157	–159	30.4
OT-15-4	24.096	121.178	2095	4	–187	–193	–186	–189	30.0
OT-15-7	24.186	121.326	2429	4	–186	–191	–184	–187	28.8
OT-15-8	24.181	121.308	2660	3	–206	–204	–196	–200	29.9
OT-15-6	24.164	121.288	2976	5	–249	–230	–223	–231	29.8
OT-15-5	24.135	121.281	3415	4	–242	–229	–226	–231	29.2

TABLE 3 | Modern Taiwan river sediment *n*-alkane δ^2H, sample elevation, and basin mean elevation.

Sample	Latitdue	Longitude	Sample Elevation	Catchment Mean Elevation	δ^2H_{nC27}	δ^2H_{nC29}	δ^2H_{nC31}	$\delta^2H_{nC27-31}$
OT-13-3	23.785	121.014	474	2151	—	–181	–175	–178
WT-11-12	121.049	23.158	778	1397	–167	–184	–174	–179
WT-11-10	121.018	23.185	782	2107	–168	–177	–175	–175
WH02	120.928	22.729	788	1516	—	–182	–170	–174
OT-14-09	120.9	22.714	1759	1956	–183	–183	–183	–183
WT-14-07A	120.883	22.731	1966	2029	–193	–185	–187	–187
OT-14-08	120.886	22.737	2013	2091	–166	–184	–176	–178
WT-11-4	121.024	23.327	2681	3005	–228	–220	–217	–220
WT-11-02	121.026	23.328	2693	2998	–217	–211	–207	–210
WT-11-03	121.025	23.327	2709	3039	–210	–216	–205	–207
WT-11-01	121.025	23.328	2709	3007	–210	–209	–207	–209
WT-11-07	121.03	23.286	3091	3228	–218	–214	–209	–213
WT-11-6	121.042	23.293	3136	3332	–217	–210	–209	–211
WT-11-05	121.054	23.293	3031	3201	–215	–207	–213	–214
19TW-LW16-Sedi	121.495	24.182	443	1600	–198	–174	–165	–179
MT-TW-07c	24.069	120.781	224	390	—	–166	–164	–165.6

cooler conditions. If changes in primary production as a function of elevation are offset by changes in degradation, it could yield a uniform effective production function across elevation ranges in an orogen.

(3) Erosion function: Organic biomarkers make their way into river sediments through a combination of ablation from leaves, transport in surface or groundwater and soil erosion. Soil erosion rates commonly scale with slope

(Braun et al., 2001; Heimsath et al., 2001) and mass wasting is often a function of relief. Thus, variations in slope throughout a catchment could impart an elevation-dependent bias on organic export. However, sediment generation and transport is not the same as organic molecular generation and transport and contributions will be controlled by a combination of biomass production and soil storage.

(4) Detrital Contribution: Ancient sediments, and in particular, clay-bearing sediments, can contain a significant reservoir of molecular compounds identical to modern plant or microbially-produced biomarkers. Detrital inputs of molecular components are generally of minimal significance in igneous terrain, however of greater concern during stages of orogenesis where there may be significant thin skin deformation and erosion of foreland sediments.

(5) Local and integrated sampling sites: For quantification of paleorelief, reconstructions must incorporate records of low elevation local (*in situ*) water isotopes as well as catchment-integrated signals or models that can approximate both. An example may be a system that is dominated by local inputs for the bulk of time, punctuated by sporadic mass wasting or erosive events. A second example could be a scenario characterized by beds of paleobotanical remains in low elevation floodplain sites (intact fossil leaf materials) in combination with sediment-bound leaf waxes. This is due to the fact that leaf transport studies show that intact leaves preserved in sedimentary sequences generally indicate short transport distances on the order of 100s of meters or less prior to deposition. Longer transport distances are commonly associated with greater degradation and breakage of intact leaves. In contrast, fine-grained sediments that contain leaf waxes bound to mineral (clay) surfaces, may be readily transported long distances. Thus comparison of waxes from intact leaf mats relative to fine grained sediments, may provide one measure of catchment relief.

(6) Elevation-dependent isotope and/or temperature relationships and constant or known fractionations between ambient water and molecular biomarkers. In order to reliably apply an organic molecular paleohypsometry approach, there must be a consistent elevation-dependent geochemical signature and a means of quantifying or constraining the relationship between that signature and organic biomarkers (for plant wax δ^2H_{nC29} this is the apparent fractionation). This relates to the factors that control signal generation.

In total, determination of catchment paleohypsometry requires attention to the key factors identified above. In addition, in order to determine a catchment-wide organic molecular hypsometry, one must assume that: 1) The production of molecular biomarkers is at steady-state at the catchment scale; and 2) Each eroding area of the catchment contributes plant- or microbial-derived biomarkers to the river sediment in proportion to the above defined production, erosion and degradation functions. In practice, it is likely that different climatic/tectonic/erosive regimes will be characterized by distinct relationships between the geochemical signature of organic matter integration and catchment hypsometry. Thus, the relationships observed in Taiwan may not readily translate to every global orogen. In addition, we note that there is a distinct difference between hypsometry and topography and comment that organic molecular hypsometry provides insight into the elevation distribution of source organics in a catchment—it does not specifically record the maximum elevation of an orogen. However, the approach presented above provides a framework for interrogation of fluvially-exported sediments as a record of the topographic evolution of an orogen and the catchments that drain a landscape.

CONCLUSION

We discuss a new approach to investigating the topographic evolution of an orogen using the isotopic signature of plant waxes preserved in fluvial deposits. Modern plant biomarker and water isotope data from Taiwan show that the $\delta^2H_{n\text{-alkane}}$ of fluvially-transported leaf waxes reflects the hypsometry of organic matter produced throughout a catchment. The isotopic composition of exported waxes is generally consistent with the $\delta^2H_{n\text{-alkane}}$ value observed at the catchment mean elevation. As a result, the $\delta^2H_{n\text{-alkane}}$ of detrital organics in fluvially-transported sediments can theoretically provide a record of catchment hypsometry through time. Models for different catchment molecular production and erosion functions show that differences in these factors can shape the relationship between the isotopic signature of fluvially-exported leaf waxes and catchment morphology, yet in our test case the effect of these varied functions is on the order of only several per mil and several hundred meters for highly distinct boundary conditions. Application of this methodology in other orogens will require further investigation of the controls on biomarker integration. Despite this, data presented here demonstrates the potential utility of organic molecular paleohypsometry as a new tool for interrogating the evolution of global orogens.

DATA AVAILABILITY STATEMENT

The original contributions presented in the study are included in the article/**Supplementary Material**, further inquiries can be directed to the corresponding author.

AUTHOR CONTRIBUTIONS

MH conceived the idea, collected and analyzed samples, and wrote the article. WO contributed to field sampling, data analysis and writing the article.

FUNDING

National Science Foundation CAREER 1752815 to MH.

SUPPLEMENTARY MATERIAL

The Supplementary Material for this article can be found online at: https://www.frontiersin.org/articles/10.3389/feart.2021.665324/full#supplementary-material

REFERENCES

Aichner, B., Feakins, S. J., Lee, J. E., Herzschuh, U., and Liu, X. (2015). High-resolution Leaf Wax Carbon and Hydrogen Isotopic Record of the Late Holocene Paleoclimate in Arid Central Asia. *Clim. Past* 11 (4), 619–633. doi:10.5194/cp-11-619-2015

Amthor, J. S., and Baldocchi, D. D. (2001). "Terrestrial Higher Plant Respiration and Net Primary Production," in *Terrestrial Global Productivity*. Editors J. Roy, B. Saugier, and H. A. Mooney (Academic Press), 33–59. doi:10.1016/b978-012505290-0/50004-1

Anderson, V. J., Saylor, J. E., Shanahan, T. M., and Horton, B. K. (2015). Paleoelevation Records from Lipid Biomarkers: Application to the Tropical Andes. *Geol. Soc. America Bull.* 127, 1604–1616. doi:10.1130/b31105.1

Axelrod, D. I. (1997). Paleoelevation Estimated from Tertiary Floras. *Int. Geology. Rev.* 39 (12), 1124–1133. doi:10.1080/00206819709465319

Bai, Y., Chen, C., Fang, X., Liu, X., and Guo, H. (2017). Altitudinal Effect of Soil N-Alkane δD Values on the Eastern Tibetan Plateau and Their Increasing Isotopic Fractionation with Altitude. *Sci. China Earth Sci.* 60 (9), 1664–1673. doi:10.1007/s11430-016-9055-4

Bai, Y., Fang, X., Jia, G., Sun, J., Wen, R., and Ye, Y. (2015). Different Altitude Effect of Leaf Wax N -alkane δD Values in Surface Soils along Two Vapor Transport Pathways, southeastern Tibetan Plateau. *Geochimica et Cosmochimica Acta* 170, 94–107. doi:10.1016/j.gca.2015.08.016

Barthlott, W., and Neinhuis, C. (1997). Purity of the Sacred lotus, or Escape from Contamination in Biological Surfaces. *Planta* 202 (1), 1–8. doi:10.1007/s004250050096

Bershaw, J., Cassel, E. J., Carlson, T. B., Streig, A. R., and Streck, M. J. (2019). Volcanic Glass as a Proxy for Cenozoic Elevation and Climate in the Cascade Mountains, Oregon, USA. *J. Volcanology Geothermal Res.* 381, 157–167. doi:10.1016/j.jvolgeores.2019.05.021

Bershaw, J., Penny, S. M., and Garzione, C. N. (2012). Stable Isotopes of Modern Water across the Himalaya and Eastern Tibetan Plateau: Implications for Estimates of Paleoelevation and Paleoclimate. *J. Geophys. Res.* 117 (D2), a–n. doi:10.1029/2011JD016132

Bierman, P. R. (1994). Using *In Situ* Produced Cosmogenic Isotopes to Estimate Rates of Landscape Evolution: A Review from the Geomorphic Perspective. *J. Geophys. Res.* 99 (B7), 13885–13896. doi:10.1029/94jb00459

Bierman, P., and Steig, E. J. (1996). Estimating Rates of Denudation Using Cosmogenic Isotope Abundances in Sediment. *Earth Surf. Process. Landforms* 21 (2), 125–139. doi:10.1002/(sici)1096-9837(199602)21:2<125:aid-esp511>3.0.co;2-8

Bliedtner, M., Zech, R., Zech, J., Schäfer, I., and Suchodoletz, H. (2020). A First Holocene Leaf Wax Isotope-based Paleoclimate Record from the Semi-humid to Semi-arid South-eastern Caucasian Lowlands. *J. Quat. Sci.* 35 (5), 625–633. doi:10.1002/jqs.3210

Botsyun, S., Sepulchre, P., Donnadieu, Y., Risi, C., Licht, A., and Caves Rugenstein, J. K. (2019). Revised Paleoaltimetry Data show low Tibetan Plateau Elevation during the Eocene. *Science* 363 (6430), eaaq1436. doi:10.1126/science.aaq1436

Botsyun, S., Sepulchre, P., Risi, C., and Donnadieu, Y. (2016). Impacts of Tibetan Plateau Uplift on Atmospheric Dynamics and Associated Precipitation δ18O. *Clim. Past* 12 (6), 1401–1420. doi:10.5194/cp-12-1401-2016

Braun, J., Heimsath, A. M., Chappell, J., and John, C. (2001). Sediment Transport Mechanisms on Soil-Mantled Hillslopes. *Geol.* 29 (8), 683. doi:10.1130/0091-7613(2001)029<0683:stmosm>2.0.co;2

Brittingham, A., Hren, M. T., and Hartman, G. (2017). Microbial Alteration of the Hydrogen and Carbon Isotopic Composition of N-Alkanes in Sediments. *Org. Geochem.* 107, 1–8. doi:10.1016/j.orggeochem.2017.01.010

Cassel, E. J., Graham, S. A., and Chamberlain, C. P. (2009). Cenozoic Tectonic and Topographic Evolution of the Northern Sierra Nevada, California, through Stable Isotope Paleoaltimetry in Volcanic Glass. *Geology* 37 (6), 547–550. doi:10.1130/g25572a.1

Chang, Q., Hren, M., Lin, A. T., Tabor, C., Yu, S.-W., Eley, Y., et al. (2021). Terrestrial Biomarker Isotope Records of Late Quaternary Climate and Source-To-Sink Sediment Transport Processes in Southwestern Taiwan. *Am. J. Sci.* 321, 393–423. doi:10.2475/04.2021.01

Chikaraishi, Y., and Naraoka, H. (2003). Compound-specific δD-δ13C Analyses of N-Alkanes Extracted from Terrestrial and Aquatic Plants. *Phytochemistry* 63 (3), 361–371. doi:10.1016/s0031-9422(02)00749-5

Chikaraishi, Y., Naraoka, H., and Poulson, S. R. (2004). Hydrogen and Carbon Isotopic Fractionations of Lipid Biosynthesis Among Terrestrial (C3, C4 and CAM) and Aquatic Plants. *Phytochemistry* 65 (10), 1369–1381. doi:10.1016/j.phytochem.2004.03.036

Clark, M. K. (2007). The Significance of Paleotopography. *Rev. Mineralogy Geochem.* 66 (1), 1–21. doi:10.2138/rmg.2007.66.1

Colwyn, D. A., Brandon, M. T., Hren, M. T., Hourigan, J., Pacini, A., Cosgrove, M. G., et al. (2019). Growth and Steady State of the Patagonian Andes. *Am. J. Sci.* 319 (6), 431–472. doi:10.2475/06.2019.01

Colwyn, D. A., and Hren, M. T. (2019). An Abrupt Decrease in Southern Hemisphere Terrestrial Temperature during the Eocene-Oligocene Transition. *Earth Planet. Sci. Lett.* 512, 227–235. doi:10.1016/j.epsl.2019.01.052

Currie, B. S., Polissar, P. J., Rowley, D. B., Ingalls, M., Li, S., Olack, G., et al. (2016). Multiproxy Paleoaltimetry of the Late Oligocene-Pliocene Oiyug Basin, Southern Tibet. *Am. J. Sci.* 316 (5), 401–436. doi:10.2475/05.2016.01

Dadson, S. J., Hovius, N., Chen, H., Dade, W. B., Hsieh, M.-L., Willett, S. D., et al. (2003). Links between Erosion, Runoff Variability and Seismicity in the Taiwan Orogen. *Nature* 426 (6967), 648–651. doi:10.1038/nature02150

Dansgaard, W. (1964). Stable Isotopes in Precipitation. *Tell'Us* 16 (4), 436–468. doi:10.1111/j.2153-3490.1964.tb00181.x

DeCelles, P. G., and Giles, K. A. (1996). Foreland basin Systems. *Basin Res.* 8 (2), 105–123. doi:10.1046/j.1365-2117.1996.01491.x

Deffontaines, B., Lee, J.-C., Angelier, J., Carvalho, J., and Rudant, J.-P. (1994). New Geomorphic Data on the Active Taiwan Orogen: a Multisource Approach. *J. Geophys. Res.* 99 (B10), 20243–20266. doi:10.1029/94jb00733

Derrieux, F., Siame, L. L., Bourlès, D. L., Chen, R.-F., Braucher, R., Léanni, L., et al. (2014). How Fast Is the Denudation of the Taiwan Mountain belt? Perspectives from *In Situ* Cosmogenic 10Be. *J. Asian Earth Sci.* 88, 230–245. doi:10.1016/j.jseaes.2014.03.012

Dettman, D. L., Fang, X., Garzione, C. N., and Li, J. (2003). Uplift-driven Climate Change at 12 Ma: a Long δ18O Record from the NE Margin of the Tibetan Plateau. *Earth Planet. Sci. Lett.* 214 (1–2), 267–277. doi:10.1016/s0012-821x(03)00383-2

Dosseto, A., and Schaller, M. (2016). The Erosion Response to Quaternary Climate Change Quantified Using Uranium Isotopes and *In Situ* - Produced Cosmogenic Nuclides. *Earth-Science Rev.* 155, 60–81. doi:10.1016/j.earscirev.2016.01.015

Ehleringer, J. R., White, J. W., Johnson, D. A., and Brick, M. (1990). Carbon Isotope Discrimination, Photosynthetic Gas Exchange and Transpiration Efficiency in Beans and Range Grasses. *Acta Oecologica* 11 (4), 611–625.

Fan, M., Constenius, K. N., and Dettman, D. L. (2017). Prolonged High Relief in the Northern Cordilleran Orogenic Front during Middle and Late Eocene Extension Based on Stable Isotope Paleoaltimetry. *Earth Planet. Sci. Lett.* 457, 376–384. doi:10.1016/j.epsl.2016.10.038

Feakins, S. J., Bentley, L. P., Salinas, N., Shenkin, A., Blonder, B., Goldsmith, G. R., et al. (2016). Plant Leaf Wax Biomarkers Capture Gradients in Hydrogen Isotopes of Precipitation from the Andes and Amazon. *Geochimica et Cosmochimica Acta* 182, 155–172. doi:10.1016/j.gca.2016.03.018

Feakins, S. J., Wu, M. S., Ponton, C., Galy, V., and West, A. J. (2018). Dual Isotope Evidence for Sedimentary Integration of Plant Wax Biomarkers across an Andes-Amazon Elevation Transect. *Geochimica et Cosmochimica Acta* 242, 64–81. doi:10.1016/j.gca.2018.09.007

Feng, R., Poulsen, C. J., Werner, M., Chamberlain, C. P., Mix, H. T., and Mulch, A. (2013). Early Cenozoic Evolution of Topography, Climate, and Stable Isotopes in Precipitation in the North American Cordillera. *Am. J. Sci.* 313 (7), 613–648. doi:10.2475/07.2013.01

Forest, C. E., Wolfe, J. A., Molnar, P., and Emanuel, K. A. (1999). Paleoaltimetry Incorporating Atmospheric Physics and Botanical Estimates of Paleoclimate. *Geol. Soc. America Bull.* 111 (4), 497–511. doi:10.1130/0016-7606(1999)111<0497:piapab>2.3.co;2

Galewsky, J. (2009). Rain Shadow Development during the Growth of Mountain Ranges: An Atmospheric Dynamics Perspective. *J. Geophys. Res.* 114 (F1), F01018. doi:10.1029/2008jf001085

Galy, V., Eglinton, T., France-Lanord, C., and Sylva, S. (2011). The Provenance of Vegetation and Environmental Signatures Encoded in Vascular Plant Biomarkers Carried by the Ganges–Brahmaputra Rivers. *Earth Planet. Sci. Lett.* 304 (1), 1–12. doi:10.1016/j.epsl.2011.02.003

Garzione, C. N., Quade, J., DeCelles, P. G., and English, N. B. (2000). Predicting Paleoelevation of Tibet and the Himalaya from δ18O vs. Altitude Gradients in

Meteoric Water across the Nepal Himalaya. *Earth Planet. Sci. Lett.* 183, 215–229. doi:10.1016/s0012-821x(00)00252-1

Ghosh, P., Garzione, C. N., and Eiler, J. M. (2006). Rapid Uplift of the Altiplano Revealed through 13C-18O Bonds in Paleosol Carbonates. *Science* 311 (5760), 511–515. doi:10.1126/science.1119365

Giustini, F., Brilli, M., and Patera, A. (2016). Mapping Oxygen Stable Isotopes of Precipitation in Italy. *J. Hydrol. Reg. Stud.* 8, 162–181. doi:10.1016/j.ejrh.2016.04.001

Gonfiantini, R., Roberto, G., Michel-Alain, R., Jean-Claude, O., Jean-Charles, F., and Zuppi, G. M. (2001). The Altitude Effect on the Isotopic Composition of Tropical rains. *Chem. Geology* 181 (1-4), 147–167. doi:10.1016/s0009-2541(01)00279-0

Granger, D. E., Kirchner, J. W., and Finkel, R. (1996). Spatially Averaged Long-Term Erosion Rates Measured from In Situ-Produced Cosmogenic Nuclides in Alluvial Sediment. *J. Geology* 104 (3), 249–257. doi:10.1086/629823

Grujic, D., Govin, G., Barrier, L., Bookhagen, B., Coutand, I., Cowan, B., et al. (2018). Formation of a Rain Shadow: O and H Stable Isotope Records in Authigenic Clays from the Siwalik Group in Eastern Bhutan. *Geochem. Geophys. Geosyst.* 19, 3430–3447. doi:10.1029/2017GC007254

Hayes, J. M. (1993). Factors Controlling 13C Contents of Sedimentary Organic Compounds: Principles and Evidence. *Mar. Geology* 113 (1-2), 111–125. doi:10.1016/0025-3227(93)90153-m

Heimsath, A. M., Dietrich, W. E., Nishiizumi, K., and Finkel, R. C. (2001). Stochastic Processes of Soil Production and Transport: Erosion Rates, Topographic Variation and Cosmogenic Nuclides in the Oregon Coast Range. *Earth Surf. Process. Landforms* 26 (5), 531–552. doi:10.1002/esp.209

Hepp, J., Tuthorn, M., Zech, R., Mügler, I., Schlütz, F., Zech, W., et al. (2015). Reconstructing lake Evaporation History and the Isotopic Composition of Precipitation by a Coupled δ18O-δ2H Biomarker Approach. *J. Hydrol.* 529, 622–631. doi:10.1016/j.jhydrol.2014.10.012

Ho, C. S. (1986). A Synthesis of the Geologic Evolution of Taiwan. *Tectonophysics* 125 (1), 1–16. doi:10.1016/0040-1951(86)90004-1

Hoffmann, B., Feakins, S. J., Bookhagen, B., Olen, S. M., Adhikari, D. P., Mainali, J., et al. (2016). Climatic and Geomorphic Drivers of Plant Organic Matter Transport in the Arun River, E Nepal. *Earth Planet. Sci. Lett.* 452 (Suppl. C), 104–114. doi:10.1016/j.epsl.2016.07.008

Hoke, G. D., Aranibar, J. N., Viale, M., Araneo, D. C., and Llano, C. (2013). Seasonal Moisture Sources and the Isotopic Composition of Precipitation, Rivers, and Carbonates across the Andes at 32.5-35.5°S. *Geochem. Geophys. Geosyst.* 14 (4), 962–978. doi:10.1002/ggge.20045

Hoke, G. D., Liu-Zeng, J., Hren, M. T., Wissink, G. K., and Garzione, C. N. (2014). Stable Isotopes Reveal High Southeast Tibetan Plateau Margin since the Paleogene. *Earth Planet. Sci. Lett.* 394, 270–278. doi:10.1016/j.epsl.2014.03.007

Holloway, P. J. (1969). The Effects of Superficial Wax on Leaf Wettability. *Ann. Appl. Biol.* 63 (1), 145–153. doi:10.1111/j.1744-7348.1969.tb05475.x

Hou, J., D'Andrea, W. J., and Huang, Y. (2008). Can Sedimentary Leaf Waxes Record D/H Ratios of continental Precipitation? Field, Model, and Experimental Assessments. *Geochimica et Cosmochimica Acta* 72 (14), 3503–3517. doi:10.1016/j.gca.2008.04.030

Hovius, N., Stark, C. P., Hao-Tsu, C., and Jiun-Chuan, L. (2000). Supply and Removal of Sediment in a Landslide-Dominated Mountain Belt: Central Range, Taiwan. *J. Geology* 108 (1), 73–89. doi:10.1086/314387

Hren, M. T., Bookhagen, B., Blisniuk, P. M., Booth, A. L., and Chamberlain, C. P. (2009). δ18O and δD of Streamwaters across the Himalaya and Tibetan Plateau: Implications for Moisture Sources and Paleoelevation Reconstructions. *Earth Planet. Sci. Lett.* 288 (1), 20–32. doi:10.1016/j.epsl.2009.08.041

Hren, M. T., Pagani, M., Erwin, D. M., and Brandon, M. (2010). Biomarker Reconstruction of the Early Eocene Paleotopography and Paleoclimate of the Northern Sierra Nevada. *Geology* 38 (1), 7–10. doi:10.1130/g30215.1

Huntington, K. W., Saylor, J., Quade, J., and Hudson, A. M. (2015). High Late Miocene-Pliocene Elevation of the Zhada Basin, Southwestern Tibetan Plateau, from Carbonate Clumped Isotope Thermometry. *Geol. Soc. America Bull.* 127, 181–199. doi:10.1130/b31000.1

Ingraham, N. L., and Taylor, B. E. (1991). Light Stable Isotope Systematics of Large-Scale Hydrologic Regimes in California and Nevada. *Water Res. Res.* 27 (1), 77–90.

Insel, N., Poulsen, C. J., and Ehlers, T. A. (2010). Influence of the Andes Mountains on South American Moisture Transport, Convection, and Precipitation. *Clim. Dyn.* 35 (7), 1477–1492. doi:10.1007/s00382-009-0637-1

Insel, N., Poulsen, C. J., Ehlers, T. A., and Sturm, C. (2012). Response of Meteoric δ18O to Surface Uplift - Implications for Cenozoic Andean Plateau Growth. *Earth Planet. Sci. Lett.* 317-318, 262–272. doi:10.1016/j.epsl.2011.11.039

Insel, N., Poulsen, C. J., Sturm, C., and Ehlers, T. A. (2013). Climate Controls on Andean Precipitation δ18O Interannual Variability. *J. Geophys. Res. Atmos.* 118 (17), 9721–9742. doi:10.1002/jgrd.50619

Jia, G., Wei, K., Chen, F., and Peng, P. a. (2008). Soil N-Alkane δD vs. Altitude Gradients along Mount Gongga, China. *Geochimica et Cosmochimica Acta* 72 (21), 5165–5174. doi:10.1016/j.gca.2008.08.004

Kent-Corson, M. L., Sherman, L. S., Mulch, A., and Chamberlain, C. P. (2006). Cenozoic Topographic and Climatic Response to Changing Tectonic Boundary Conditions in Western North America. *Earth Planet. Sci. Lett.* 252 (3–4), 453–466. doi:10.1016/j.epsl.2006.09.049

Kirkels, F. M. S. A., Ponton, C., Galy, V., West, A. J., Feakins, S. J., Peterse, F., et al. (2020). From Andes to Amazon: Assessing Branched Tetraether Lipids as Tracers for Soil Organic Carbon in the Madre de Dios River System. *J. Geophys. Res. Biogeosci.* 125 (Issue 1). doi:10.1029/2019jg005270

Kohn, M. J., Miselis, J. L., and Fre, T. J. (2002). Oxygen Isotope Evidence for Progressive Uplift of the Cascade Range, Oregon. *Earth Planet. Sci. Lett.* 204 (1-2), 151–165. doi:10.1016/s0012-821x(02)00961-5

Kohn, M. J. (2018). Paleoaltimetry: Geochemical and Thermodynamic Approaches, in *Mineralogy & Geochemistry* (Walter de Gruyter GmbH & Co KG), Vol. 66.

Kutzbach, J. E., Guetter, P. J., Ruddiman, W. F., and Prell, W. L. (1989). Sensitivity of Climate to Late Cenozoic Uplift in Southern Asia and the American West: Numerical Experiments. *J. Geophys. Res.* 94 (D15), 18393. doi:10.1029/jd094id15p18393

Lechler, A. R., and Galewsky, J. (2013). Refining Paleoaltimetry Reconstructions of the Sierra Nevada, California, Using Air Parcel Trajectories. *Geology* 41 (2), 259–262. doi:10.1130/g33553.1

Lee, T.-Y., Huang, J.-C., Lee, J.-Y., Jien, S.-H., Zehetner, F., and Kao, S.-J. (2015). Magnified Sediment Export of Small Mountainous Rivers in Taiwan: Chain Reactions from Increased Rainfall Intensity under Global Warming. *PLoS One* 10 (9), e0138283. doi:10.1371/journal.pone.0138283

Lee, Y.-H., Chen, C.-C., Liu, T.-K., Ho, H.-C., Lu, H.-Y., and Lo, W. (2006). Mountain Building Mechanisms in the Southern Central Range of the Taiwan Orogenic Belt—From Accretionary Wedge Deformation to Arc--continental Collision. *Earth Planet. Sci. Lett.* 252 (3-4), 413–422. doi:10.1016/j.epsl.2006.09.047

Li, L., Fan, M., Davila, N., Jesmok, G., Mitsunaga, B., Tripati, A., et al. (2019). Carbonate Stable and Clumped Isotopic Evidence for Late Eocene Moderate to High Elevation of the East-central Tibetan Plateau and its Geodynamic Implications. *GSA Bull.* 131, 831–844. doi:10.1130/b32060.1

Li, L., and Garzione, C. N. (2017). Spatial Distribution and Controlling Factors of Stable Isotopes in Meteoric Waters on the Tibetan Plateau: Implications for Paleoelevation Reconstruction. *Earth Planet. Sci. Lett.* 460, 302–314. doi:10.1016/j.epsl.2016.11.046

Liu, J., and An, Z. (2019). Variations in Hydrogen Isotopic Fractionation in Higher Plants and Sediments across Different Latitudes: Implications for Paleohydrological Reconstruction. *Sci. Total Environ.* 650, 470–478. doi:10.1016/j.scitotenv.2018.09.047

Liu, J., Liu, W., An, Z., and Yang, H. (2016). Different Hydrogen Isotope Fractionations during Lipid Formation in Higher Plants: Implications for Paleohydrology Reconstruction at a Global Scale. *Sci. Rep.* 6, 19711. doi:10.1038/srep19711

Malhi, Y., Girardin, C. A. J., Goldsmith, G. R., Doughty, C. E., Salinas, N., Metcalfe, D. B., et al. (2017). The Variation of Productivity and its Allocation along a Tropical Elevation Gradient: a Whole Carbon Budget Perspective. *New Phytol.* 214 (3), 1019–1032. doi:10.1111/nph.14189

Molnar, P., Houseman, G. A., and England, P. C. (2006). Palaeo-altimetry of Tibet. *Nature* 444 (7117), E4. doi:10.1038/nature05368

Mulch, A., and Chamberlain, C. P. (2007). Stable Isotope Paleoaltimetry in Orogenic Belts the Silicate Record in Surface and Crustal Geological Archives. *Rev. Mineralogy Geochem.* 66 (1), 89–118. doi:10.2138/rmg.2007.66.4

Mulch, A., Teyssier, C., Cosca, M. A., and Chamberlain, C. P. (2007). Stable Isotope Paleoaltimetry of Eocene Core Complexes in the North American Cordillera. *Tectonics* 26 (4), TC4001. doi:10.1029/2006tc001995

National Academies of Sciences, Engineering, and Medicine (2020). Division on Earth and Life Studies, Board on Earth Sciences and Resources, & Committee

on Catalyzing Opportunities for Research in the Earth Sciences (CORES): A Decadal Survey for NSFâ¬"s Division of Earth Sciences. *A Vision for NSF Earth Sciences 2020-2030: Earth in Time*. Washington, DC: National Academies Press.

Nieto-Moreno, V., Rohrmann, A., van der Meer, M. T. J., Sinninghe Damsté, J. S., Sachse, D., Tofelde, S., et al. (2016). Elevation-dependent Changes in N -alkane δ D and Soil GDGTs across the South Central Andes. *Earth Planet. Sci. Lett.* 453, 234–242. doi:10.1016/j.epsl.2016.07.049

Norris, R. D., Jones, L. S., Corfield, R. M., and Cartlidge, J. E. (1996). Skiing in the Eocene Uinta Mountains? Isotopic Evidence in the Green River Formation for Snow Melt and Large Mountains. *Geol.* 24 (5), 403. doi:10.1130/0091-7613(1996)024<0403:siteum>2.3.co;2

Page Chamberlain, C., and Poage, M. A. (2000). Reconstructing the Paleotopography of Mountain Belts from the Isotopic Composition of Authigenic Minerals. *Geology* 28 (2), 115–118. doi:10.1130/0091-7613(2000)028<0115:rtpomb>2.3.co;2

Phillips, M. J., Page, T. J., de Bruyn, M., Huey, J. A., Humphreys, W. F., Hughes, J. M., et al. (2013). The Linking of Plate Tectonics and Evolutionary Divergence. *Curr. Biol.* 23 (14), R603–R605. doi:10.1016/j.cub.2013.06.001

Poage, M. A., and Chamberlain, C. P. (2001). Empirical Relationships between Elevation and the Stable Isotope Composition of Precipitation and Surface Waters: Considerations for Studies of Paleoelevation Change. *Am. J. Sci.* 301 (1), 1–15. doi:10.2475/ajs.301.1.1

Poage, M. A., and Chamberlain, C. P. (2002). Stable Isotopic Evidence for a Pre-middle Miocene Rain Shadow in the Western Basin and Range: Implications for the Paleotopography of the Sierra Nevada. *Tectonics* 21 (4), 16–10. doi:10.1029/2001tc001303

Polissar, P. J., Freeman, K. H., Rowley, D. B., McInerney, F. A., and Currie, B. S. (2009). Paleoaltimetry of the Tibetan Plateau from D/H Ratios of Lipid Biomarkers. *Earth Planet. Sci. Lett.* 287 (1–2), 64–76. doi:10.1016/j.epsl.2009.07.037

Ponton, C., West, A. J., Feakins, S. J., and Galy, V. (2014). Leaf Wax Biomarkers in Transit Record River Catchment Composition. *Geophys. Res. Lett.* 41 (18), 6420–6427. doi:10.1002/2014gl061328

Poulsen, C. J., Ehlers, T. A., and Insel, N. (2010). Onset of Convective Rainfall during Gradual Late Miocene Rise of the central Andes. *Science* 328 (5977), 490–493. doi:10.1126/science.1185078

Quade, J., Breecker, D. O., Daëron, M., and Eiler, J. (2011). The Paleoaltimetry of Tibet: An Isotopic Perspective. *Am. J. Sci.* 311 (2), 77–115. doi:10.2475/02.2011.01

Quade, J., Eiler, J., Daëron, M., and Achyuthan, H. (2013). The Clumped Isotope Geothermometer in Soil and Paleosol Carbonate. *Geochimica et Cosmochimica Acta* 105, 92–107. doi:10.1016/j.gca.2012.11.031

Quade, J., Garzione, C., and Eiler, J. (2007). Paleoelevation Reconstruction Using Pedogenic Carbonates. *Rev. Mineralogy Geochem.* 66 (1), 53–87. doi:10.2138/rmg.2007.66.3

Quezadas, J. P., Silva, A. C., Inguaggiato, S., Ortegadel, M. d. R. S. R. S., Pérez, J. C., and Heilweil, V. M. (2015). Meteoric Isotopic Gradient on the Windward Side of theSierra Madre Oriental Area, Veracruz - Mexico. *Geofísica Internacional* 54 (3), 267–276. doi:10.1016/j.gi.2015.04.021

Ramstein, G., Fluteau, F., Besse, J., and Joussaume, S. (1997). Effect of Orogeny, Plate Motion and Land-Sea Distribution on Eurasian Climate Change over the Past 30 Million Years. *Nature* 386 (6627), 788–795. doi:10.1038/386788a0

Roe, G. H. (2005). OROGRAPHIC PRECIPITATION. *Annu. Rev. Earth Planet. Sci.* 33 (1), 645–671. doi:10.1146/annurev.earth.33.092203.122541

Roe, G. H., Stolar, D. B., and Willett, S. D. (2006). Response of a Steady-State Critical Wedge Orogen to Changes in Climate and Tectonic Forcing. *SPECIAL PAPERS-GEOLOGICAL SOCIETY AMERICA* 398, 227. doi:10.1130/2005.2398(13)

Rohrmann, A., Sachse, D., Mulch, A., Pingel, H., Tofelde, S., Alonso, R. N., et al. (2016). Miocene Orographic Uplift Forces Rapid Hydrological Change in the Southern central Andes. *Sci. Rep.* 6, 35678. doi:10.1038/srep35678

Rowley, D. B., and Currie, B. S. (2006). Palaeo-altimetry of the Late Eocene to Miocene Lunpola basin, central Tibet. *Nature* 439 (7077), 677–681. doi:10.1038/nature04506

Rowley, D. B., and Garzione, C. N. (2007). Stable Isotope-Based Paleoaltimetry. *Annu. Rev. Earth Planet. Sci.* 35 (1), 463–508. doi:10.1146/annurev.earth.35.031306.140155

Rowley, D. B. (2006). Oxygen Isotope Based Paleoaltimetry: Modern Data-Model Comparison and Paleo-Elevation History of Tibet. *Geochimica et Cosmochimica Acta* 70 (18), A541. doi:10.1016/j.gca.2006.06.999

Rowley, D. B., Pierrehumbert, R. T., and Currie, B. S. (2001). A New Approach to Stable Isotope-Based Paleoaltimetry: Implications for Paleoaltimetry and Paleohypsometry of the High Himalaya since the Late Miocene. *Earth Planet. Sci. Lett.* 188 (1-2), 253–268. doi:10.1016/s0012-821x(01)00324-7

Ruddiman, W. F., and Kutzbach, J. E. (1989). Forcing of Late Cenozoic Northern Hemisphere Climate by Plateau Uplift in Southern Asia and the American West. *J. Geophys. Res.* 94 (D15), 18409. doi:10.1029/jd094id15p18409

Ruddiman, W. F. (2013). *Tectonic Uplift and Climate Change*. Springer Science & Business Media.

Sachse, D., Billault, I., Bowen, G. J., Chikaraishi, Y., Dawson, T. E., Feakins, S. J., et al. (2012). Molecular Paleohydrology: Interpreting the Hydrogen-Isotopic Composition of Lipid Biomarkers from Photosynthesizing Organisms. *Annu. Rev. Earth Planet. Sci.* 40, 221–249. doi:10.1146/annurev-earth-042711-105535

Sachse, D., Radke, J., and Gleixner, G. (2004). Hydrogen Isotope Ratios of Recent Lacustrine Sedimentary N-Alkanes Record Modern Climate Variability. *Geochimica et Cosmochimica Acta* 68 (23), 4877–4889. doi:10.1016/j.gca.2004.06.004

Sachse, D., Radke, J., and Gleixner, G. (2006). δD Values of Individual N-Alkanes from Terrestrial Plants along a Climatic Gradient - Implications for the Sedimentary Biomarker Record. *Org. Geochem.* 37 (4), 469–483. doi:10.1016/j.orggeochem.2005.12.003

Sahagian, D. L., and Maus, J. E. (1994). Basalt Vesicularity as a Measure of Atmospheric Pressure and Palaeoelevation. *Nature* 372 (6505), 449–451. doi:10.1038/372449a0

Sahagian, D. L., Proussevitch, A. A., and Carlson, W. D. (2002). Analysis of Vesicular Basalts and Lava Emplacement Processes for Application as a Paleobarometer/Paleoaltimeter. *J. Geology* 110 (6), 671–685. doi:10.1086/342627

Sahagian, D., and Proussevitch, A. (2007). Paleoelevation Measurement on the Basis of Vesicular Basalts. *Rev. Mineralogy Geochem.* 66 (1), 195–213. doi:10.2138/rmg.2007.66.8

Saylor, J. E., Mora, A., Horton, B. K., and Nie, J. (2009). Controls on the Isotopic Composition of Surface Water and Precipitation in the Northern Andes, Colombian Eastern Cordillera. *Geochimica et Cosmochimica Acta* 73 (23), 6999–7018. doi:10.1016/j.gca.2009.08.030

Schäfer, I. K., Bliedtner, M., Wolf, D., Kolb, T., Zech, J., Faust, D., et al. (2018). A δ13C and δ2H Leaf Wax Record from the Late Quaternary Loess-Paleosoil Sequence El Paraíso, Central Spain. *Palaeogeogr. Palaeoclimatol. Palaeoecol.* 507, 52–59. doi:10.1016/j.palaeo.2018.06.039

Schaller, M., Hovius, N., Willett, S. D., Ivy-Ochs, S., Synal, H.-A., and Chen, M.-C. (2005). Fluvial Bedrock Incision in the Active Mountain belt of Taiwan Fromin Situ-Produced Cosmogenic Nuclides. *Earth Surf. Process. Landforms* 30 (8), 955–971. doi:10.1002/esp.1256

Schimmelmann, A., Lewan, M. D., Wintsch, R. P., and Wintsch, R. P. (1999). D/H Isotope Ratios of Kerogen, Bitumen, Oil, and Water in Hydrous Pyrolysis of Source Rocks Containing Kerogen Types I, II, IIS, and III. *Geochimica et Cosmochimica Acta* 63 (22), 3751–3766. doi:10.1016/s0016-7037(99)00221-5

Schimmelmann, A., Sessions, A. L., and Mastalerz, M. (2006). HYDROGEN ISOTOPIC (D/H) COMPOSITION OF ORGANIC MATTER DURING DIAGENESIS AND THERMAL MATURATION. *Annu. Rev. Earth Planet. Sci.* 34 (1), 501–533. doi:10.1146/annurev.earth.34.031405.125011

Scholl, M. A., Giambelluca, T. W., Gingerich, S. B., Nullet, M. A., and Loope, L. L. (2007). Cloud Water in Windward and Leeward Mountain Forests: The Stable Isotope Signature of Orographic Cloud Water: ISOTOPE SIGNATURE of CLOUD WATER. *Water Resour. Res.* 43 (12), 5105. doi:10.1029/2007wr006011

Scholl, M. A., Ingebritsen, S. E., Janik, C. J., and Kauahikaua, J. P. (1996). Use of Precipitation and Groundwater Isotopes to Interpret Regional Hydrology on a Tropical Volcanic Island: Kilauea Volcano Area, Hawaii. *Water Resour. Res.* 32 (12), 3525–3537. doi:10.1029/95wr02837

Shen, H., and Poulsen, C. J. (2019). Precipitation δ18O on the Himalaya-Tibet Orogeny and its Relationship to Surface Elevation. *Clim. Past* 15, 169–187. doi:10.5194/cp-15-169-2019

Siame, L. L., Angelier, J., Chen, R.-F., Godard, V., Derrieux, F., Bourlès, D. L., et al. (2011). Erosion Rates in an Active Orogen (NE-Taiwan): A Confrontation of

Cosmogenic Measurements with River Suspended Loads. *Quat. Geochronol.* 6 (2), 246–260. doi:10.1016/j.quageo.2010.11.003

Sjostrom, D. J., Hren, M. T., Horton, T. W., Waldbauer, J. R., and Chamberlain, C. P. (2006). Stable Isotopic Evidence for a Pre--late Miocene Elevation Gradient in the Great Plains--Rocky Mountain Region, USA. *Geol. Soc. America Spec. Pap.* 398, 309–319. doi:10.1130/2006.2398(19)

Smith, R. B., and Evans, J. P. (2007). Orographic Precipitation and Water Vapor Fractionation over the Southern Andes. *J. Hydrometeorology* 8 (1), 3–19. doi:10.1175/jhm555.1

Staisch, L. M., Niemi, N. A., Hong, C., Clark, M. K., Rowley, D. B., and Currie, B. (2014). A Cretaceous-Eocene Depositional Age for the Fenghuoshan Group, Hoh Xil Basin: Implications for the Tectonic Evolution of the Northern Tibet Plateau. *Tectonics* 33 (3), 2013TC003367. doi:10.1002/2013tc003367

Stern, L. A., and Blisniuk, P. M. (2002). Stable Isotope Composition of Precipitation across the Southern Patagonian Andes. *J. Geophys. Res. Atmospheres* 107 (D23), 4667. doi:10.1029/2002jd002509

Stolar, D. B., Willett, S. D., and Montgomery, D. R. (2007). Characterization of Topographic Steady State in Taiwan. *Earth Planet. Sci. Lett.* 261 (3), 421–431. doi:10.1016/j.epsl.2007.07.045

Struck, J., Bliedtner, M., Strobel, P., Bittner, L., Bazarradnaa, E., Andreeva, D., et al. (2020). Leaf Waxes and Hemicelluloses in Topsoils Reflect the δ2H and δ18O Isotopic Composition of Precipitation in Mongolia. *Front. Earth Sci.* 8, 343. doi:10.3389/feart.2020.00343

Suppe, J., Liou, J. G., and Ernst, W. G. (1981). Paleogeographic Origins of the Miocene East Taiwan Ophiolite. *Am. J. Sci.* 281 (3), 228–246. doi:10.2475/ajs.281.3.228

Tang, M., Liu-Zeng, J., Hoke, G. D., Xu, Q., Wang, W., Li, Z., et al. (2017). Paleoelevation Reconstruction of the Paleocene-Eocene Gonjo basin, SE-central Tibet. *Tectonophysics* 712-713, 170–181. doi:10.1016/j.tecto.2017.05.018

Teng, L. S. (1990). Geotectonic Evolution of Late Cenozoic Arc-Continent Collision in Taiwan. *Tectonophysics* 183 (1), 57–76. doi:10.1016/0040-1951(90)90188-e

Tipple, B. J., and Pagani, M. (2013). Environmental Control on Eastern Broadleaf forest Species' Leaf Wax Distributions and D/H Ratios. *Geochimica et Cosmochimica Acta* 111, 64–77. doi:10.1016/j.gca.2012.10.042

Tuthorn, M., Zech, R., Ruppenthal, M., Oelmann, Y., Kahmen, A., del Valle, H. F., et al. (2015). Coupling δ2H and δ18O Biomarker Results Yields Information on Relative Humidity and Isotopic Composition of Precipitation - a Climate Transect Validation Study. *Biogeosciences* 12 (12), 3913–3924. doi:10.5194/bg-12-3913-2015

Usman, M. O., Kirkels, F. M. S. A., Zwart, H. M., Basu, S., Ponton, C., Blattmann, T. M., et al. (2018). Reconciling Drainage and Receiving basin Signatures of the Godavari River System. *Biogeosciences* 15 (11), 3357–3375. doi:10.5194/bg-15-3357-2018

Valdivielso, S., Vázquez-Suñé, E., and Custodio, E. (2020). Origin and Variability of Oxygen and Hydrogen Isotopic Composition of Precipitation in the Central Andes: A Review. *J. Hydrol.* 587, 124899. doi:10.1016/j.jhydrol.2020.124899

Vogts, A., Badewien, T., Rullkötter, J., and Schefuß, E. (2016). Near-constant Apparent Hydrogen Isotope Fractionation between Leaf Wax N-Alkanes and Precipitation in Tropical Regions: Evidence from a marine Sediment Transect off SW Africa. *Org. Geochem.* 96, 18–27. doi:10.1016/j.orggeochem.2016.03.003

Wang, C., Hren, M. T., Hoke, G. D., Liu-Zeng, J., and Garzione, C. N. (2017). Soil N-Alkane δD and Glycerol Dialkyl Glycerol Tetraether (GDGT) Distributions along an Altitudinal Transect from Southwest China: Evaluating Organic Molecular Proxies for Paleoclimate and Paleoelevation. *Org. Geochem.* 107, 21–32. doi:10.1016/j.orggeochem.2017.01.006

Wang, J., Howarth, J. D., McClymont, E. L., Densmore, A. L., Fitzsimons, S. J., Croissant, T., et al. (2020). Long-term Patterns of Hillslope Erosion by Earthquake-Induced Landslides Shape Mountain Landscapes. *Sci. Adv.* 6 (23), eaaz6446. doi:10.1126/sciadv.aaz6446

Wheeler, L. B., Galewsky, J., Herold, N., and Huber, M. (2016). Late Cenozoic Surface Uplift of the Southern Sierra Nevada (California, USA): A Paleoclimate Perspective on lee-side Stable Isotope Paleoaltimetry. *Geology* 44 (6), 451–454. doi:10.1130/g37718.1

Willenbring, J. K., Gasparini, N. M., Crosby, B. T., and Brocard, G. (2013). What Does a Mean Mean? the Temporal Evolution of Detrital Cosmogenic Denudation Rates in a Transient Landscape. *Geology* 41 (12), 1215–1218. doi:10.1130/g34746.1

Willett, S. D., and Brandon, M. T. (2002). On Steady States in Mountain Belts. *Geol.* 30 (2), 175–178. doi:10.1130/0091-7613(2002)030<0175:ossimb>2.0.co;2

Wolfe, J. A., Schorn, H. E., Forest, C. E., and Molnar, P. (1997). Paleobotanical Evidence for High Altitudes in Nevada during the Miocene. *Science*, 276, 1672–1675. doi:10.1126/science.276.5319.1672

Xu, Q., Ding, L., Zhang, L., Yang, D., Cai, F., Lai, Q., et al. (2010). Stable Isotopes of Modern Herbivore Tooth Enamel in the Tibetan Plateau: Implications for Paleoelevation Reconstructions. *Chin. Sci. Bull.* 55 (1), 45–54. doi:10.1007/s11434-009-0543-2

Yang, H., and Huang, Y. (2003). Preservation of Lipid Hydrogen Isotope Ratios in Miocene Lacustrine Sediments and Plant Fossils at Clarkia, Northern Idaho, USA. *Org. Geochem.* 34 (3), 413–423. doi:10.1016/s0146-6380(02)00212-7

Yang, X., Xu, B., Yang, W., and Qu, D. (2012). The Indian Monsoonal Influence on Altitude Effect of δ 18O in Surface Water on Southeast Tibetan Plateau. *Sci. China Earth Sci.* 55, 438–445. doi:10.1007/s11430-011-4342-7

Yu, H.-S., and Chow, J. (1997). Cenozoic Basins in Northern Taiwan and Tectonic Implications for the Development of the Eastern Asian continental Margin. *Palaeogeogr. Palaeoclimatol. Palaeoecol.* 131, 133–144. doi:10.1016/s0031-0182(96)00124-1

Zech, M., Pedentchouk, N., Buggle, B., Leiber, K., Kalbitz, K., Marković, S. B., et al. (2011). Effect of Leaf Litter Degradation and Seasonality on D/H Isotope Ratios of N-Alkane Biomarkers. *Geochimica et Cosmochimica Acta* 75 (17), 4917–4928. doi:10.1016/j.gca.2011.06.006

Zech, M., Zech, R., Rozanski, K., Gleixner, G., and Zech, W. (2015). Don-alkane Biomarkers in Soils/sediments Reflect theδ2H Isotopic Composition of Precipitation? A Case Study from Mt. Kilimanjaro and Implications for Paleoaltimetry and Paleoclimate Research. *Isotopes Environ. Health Stud.* 51 (4), 508–524. doi:10.1080/10256016.2015.1058790

Zhuang, G., Pagani, M., Chamberlin, C., Strong, D., and Vandergoes, M. (2015). Altitudinal Shift in Stable Hydrogen Isotopes and Microbial Tetraether Distribution in Soils from the Southern Alps, NZ: Implications for Paleoclimatology and Paleoaltimetry. *Org. Geochem.* 79, 56–64. doi:10.1016/j.orggeochem.2014.12.007

Zhuang, G., Zhang, Y. G., Hourigan, J., Ritts, B., Hren, M., Hou, M., et al. (2019). Microbial and Geochronologic Constraints on the Neogene Paleotopography of Northern Tibetan Plateau. *Geophys. Res. Lett.* 46 (3), 1312–1319. doi:10.1029/2018gl081505

Conflict of Interest: The authors declare that the research was conducted in the absence of any commercial or financial relationships that could be construed as a potential conflict of interest.

Publisher's Note: All claims expressed in this article are solely those of the authors and do not necessarily represent those of their affiliated organizations, or those of the publisher, the editors and the reviewers. Any product that may be evaluated in this article, or claim that may be made by its manufacturer, is not guaranteed or endorsed by the publisher.